

1 **Tropical montane forest conversion is a critical driver for sediment supply in**
2 **East African catchments**

3 **Jaqueline Stenfert Kroese^{1,2}, Suzanne R. Jacobs⁴, Wlodek Tych¹, Lutz Breuer^{3,4}, John N.**
4 **Quinton¹, Mariana C. Rufino^{1,2}**

5 ¹Lancaster Environment Centre, Lancaster University, Lancaster, LA1 4YQ, United Kingdom,

6 ²Centre for International Forestry Research (CIFOR), c/o World Agroforestry Centre, United

7 Nations Avenue, Gigiri, P.O. Box 30677 – 00100 Nairobi, Kenya, ³Institute for Landscape

8 Ecology and Resources Management (ILR), Justus Liebig University, Heinrich-Buff-Ring 26,

9 35392 Giessen, Germany, ⁴Centre for International Development and Environmental Research

10 (ZEU), Justus Liebig University, Senckenbergstr. 3, 35390 Giessen, Germany

11 Corresponding author: Jaqueline Stenfert Kroese (j.stenfertkroese@lancaster.ac.uk)

12 **Key Points:**

- 13 • Agricultural catchments generated six times more suspended sediment yield than a
14 forested catchment.
- 15 • Land use change towards agriculture shifted the dominant water pathways from deep
16 subsurface to shallow subsurface flow and surface runoff.
- 17 • Delayed sediment responses were observed in a smallholder agriculture catchment, in
18 contrast to fast responses in a forested catchment.
- 19

20 **Abstract**

21 Land use change is known to affect suspended sediment fluxes in headwater catchments. There
22 is however limited empirical evidence of the magnitude of these effects for montane catchments
23 in East Africa. We collected a unique four-year high frequency dataset and assessed seasonal
24 sediment variation, water pathways and sediment response to hydrology in three catchments
25 under contrasting land use in the Mau Forest Complex, Kenya's largest tropical montane forest.
26 Annual suspended sediment yield was significantly higher in a smallholder
27 agriculture-dominated catchment ($131.5 \pm 90.6 \text{ t km}^{-2} \text{ yr}^{-1}$) than in a tea-tree plantation catchment
28 ($42.0 \pm 21.0 \text{ t km}^{-2} \text{ yr}^{-1}$) and a natural forest catchment ($21.5 \pm 11.1 \text{ t km}^{-2} \text{ yr}^{-1}$) ($p < 0.05$). Transfer
29 function models showed that in the natural forest and the tea-tree plantations subsurface flow
30 pathways delivered water to the stream, while in the smallholder agriculture shallow subsurface
31 and surface runoff were dominant. There was a delayed sediment response to rainfall for the
32 smallholder agriculture and the tea-tree plantations. A slow depletion in sediment supply
33 suggests that the wider catchment area supplies sediment, especially in the catchment dominated
34 by smallholder farming. In contrast, a fast sediment response and depletion in sediment supply in
35 the natural forest suggests a dominance of temporarily stored and nearby sediment sources. This
36 study shows that the vegetation cover of a forest ecosystem is very effective in conserving soil,
37 whereas catchments with more bare soil and poor soil conservation practices generated six times
38 more suspended sediment yield. Catchment connectivity through unpaved tracks is thought to be
39 the main explanation for the difference in sediment yield.

40 **Keywords:** Land use, temporal and spatial variability, suspended sediment, water pathways,
41 tropical montane forests, Lake Victoria basin

42 **1 Introduction**

43 The conversion of native ecosystems to agriculture leads to the degradation of soil properties
44 (Morgan 2005; Githui *et al.* 2009; Owuor *et al.* 2018), which can increase soil erosion rates
45 (Bruijnzeel 2004). Soil erosion does not only deplete fertile topsoil from agricultural land, but
46 also leads to water quality deterioration caused by an increase in fine suspended sediments
47 (Brown *et al.* 1996; Quinton *et al.* 2001; Horowitz 2008). Hence, suspended sediment physically
48 affects the fluvial network, (Owens *et al.* 2005) polluting drinking water for communities,

49 livestock and wildlife, and impacting downstream water reservoirs and hydropower generation
50 because of the accumulation of the sediments (Mogaka *et al.* 2006; Foster *et al.* 2012; Wangechi
51 *et al.* 2015). Additionally, pollutants such as pesticides (Brown *et al.* 1996) and nutrients
52 (phosphorus or nitrogen) (Fraser *et al.* 1999; Quinton *et al.* 2001; Horowitz 2008) can be
53 attached to sediments and can harm aquatic biota (Owens *et al.* 2005; Kemp *et al.* 2011; Gellis &
54 Mukundan 2013). The increase in nutrient concentrations can result in eutrophication of water
55 bodies (Foy & Bailey-Watts 1998; Hilton *et al.* 2006; Mogaka *et al.* 2006).

56 Land use change in catchments with strong connectivity between sediment sources and streams
57 can abruptly increase sediment supply to the fluvial system (Fryirs 2013). There may be multiple
58 sediment source areas, such as hillslope soils (Minella *et al.* 2008; Didoné *et al.* 2014), gullies
59 (Poesen *et al.* 2003; Minella *et al.* 2008; Fan *et al.* 2012), riverbanks (Trimble & Mendel 1995;
60 Lefrançois *et al.* 2007) and unpaved tracks (Ziegler *et al.* 2001; Minella *et al.* 2008; Ramos-
61 Scharrón & Thomaz 2016). Unravelling sediment dynamics is complex and requires continuous
62 high-frequency monitoring because suspended sediment concentrations change rapidly
63 throughout individual storms (De Girolamo *et al.* 2015; Sun *et al.* 2016; Vercruysse *et al.* 2017).
64 Alternatively, turbidity observations can be used as a surrogate to determine in-stream suspended
65 sediment concentrations, which allow for establishing continuous *in situ* suspended sediment
66 datasets, even for remote sites (Lewis 1996; Ziegler *et al.* 2014; Minella *et al.* 2018).

67 Streams in montane headwaters are major contributors to suspended sediment yield because of
68 the steep terrain that leads to a strong hillslope to channel connectivity (Wohl 2006; Grangeon *et al.*
69 *et al.* 2012; Morris 2014). Significant increases in suspended sediment yield can be expected from
70 tropical montane headwater catchments, which are heavily affected by deforestation followed by
71 cultivation of erosion prone areas, often without soil conservation measures (Ramos-Scharrón &
72 Thomaz, 2016; Wohl, 2006). Land use change may impact catchment hydrology and runoff
73 mechanisms in the tropics (Muñoz-Villers & McDonnell 2013; Ogden *et al.* 2013), which are
74 key processes determining sediment yields.

75 In East-Africa, land use change in tropical montane forests are mainly driven by scarcity of
76 arable land (Pellikka *et al.* 2004) with the most fertile lands located in the proximity of natural
77 ecosystems (Krhoda 1988). The Mau Forest Complex exemplifies this case, with one quarter of

78 the forest converted to agricultural land over the last four decades (Brandt *et al.* 2018), in
79 addition to the clearances at the beginning of the 20th century to establish commercial tea
80 plantations (Binge 1962). Due to its location in the highlands of Kenya, the Mau forest is a
81 critical catchment area for the country; it is the headwater to twelve rivers, one of which is the
82 Sondu River, a tributary of Lake Victoria (UNEP *et al.* 2005; Mogaka *et al.* 2006).

83 Eutrophication and sedimentation are major environmental problems affecting Lake Victoria,
84 where sediments are estimated to accumulate at a rate of 2.3 mm yr⁻¹ (Verschuren *et al.* 2002).
85 Although authorities in Kenya acknowledge the need to reduce sediment pollution, the linkages
86 between land use change and changes in sediment dynamics in the headwater catchments are not
87 well quantified (Nyssen *et al.* 2004; Vanmaercke *et al.* 2010, 2014). There is limited data on
88 sediment export for montane catchments in Sub-Saharan Africa in general, and in East Africa in
89 particular (Walling & Webb 1996; Ntiba *et al.* 2001). Clearly, this is a significant gap in our
90 knowledge of these environments that requires empirical measurements to address it. Not only
91 will these measurements improve our understanding of these under-researched environments, but
92 they will also assist in the development of targeted soil and water conservation strategies to
93 disconnect sediment source areas in the upper catchments of the Mau Forest from the fluvial
94 system and downstream environments, including Lake Victoria.

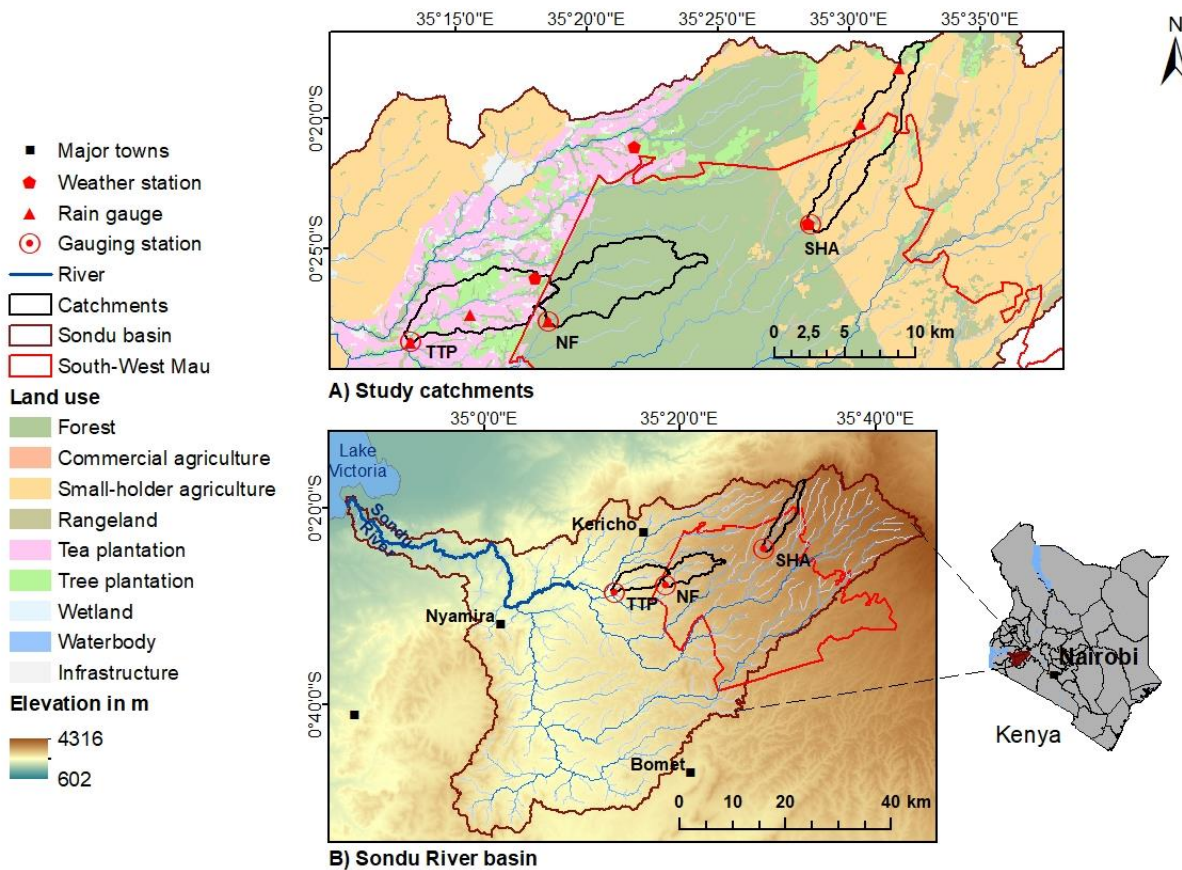
95 The overall aim of this study was to elucidate the spatial and temporal dynamics of suspended
96 sediment and to quantify suspended sediment loads in tropical montane streams under
97 contrasting land uses using a four year high-temporal resolution dataset. The main objectives
98 were: (a) to quantify rainfall, streamflow and suspended sediment transport dynamics, (b) to
99 compare the seasonal responses in suspended sediment yield, (c) to assess the timing of the
100 response of suspended sediment to rainfall and discharge and (d) to improve our understanding
101 of the dominant water flow pathways.

102 **2 Materials and Methods**

103 2.1 Catchment characteristics and site description

104 The three catchments studied are located in the headwaters of the Sondu River basin (3,470 km²)
105 in the Western Highlands of Kenya (Figure 1). Each catchment is dominated by a distinct land
106 use: (1) natural forest (NF; 35.9 km²), (2) smallholder agriculture (SHA; 27.2 km²) and (3)

107 tea-tree plantations (TTP; 33.3 km²). The Sondu River drains into Lake Victoria, which is the
 108 second largest fresh water lake in the world, an important water and economic resource for five
 109 countries and one source of the Nile River.



110
 111 Figure 1 Overview of the A) study catchments: tea-tree plantations (TTP), natural forest (NF) and the
 112 smallholder agriculture (SHA), showing locations of gauging and weather stations, tipping bucket rain
 113 gauges and land use in the B) Sondu River basin and its outlet to Lake Victoria (SRTM digital elevation
 114 model 30 m resolution; USGS, 2000) in Western Kenya.

115 The three catchments (Table 1) are characterized by steep hillslopes with a maximum slope
 116 gradient of 72% in the natural forest catchment. The streams are mostly first- and second-order
 117 perennial streams that merge together to form the River Sondu (a sixth-order stream). The rainy
 118 seasons are bimodal with a long rainy season between March and June, and a short rainy season
 119 between October and December with a continued intermediate rainy season between the two wet
 120 seasons. Mean annual precipitation is $1,988 \pm 328$ mm (period 1905-2014) with rainfall peaks in

121 April and May (>260 mm month⁻¹). January and February (<95 mm month⁻¹) are the driest
122 months.

123 Table 1 Physical characteristics of the three catchments under different land use natural forest, tea-tree
124 plantations and smallholder agriculture in the South-West Mau, Kenya.

	Natural forest	Tea-tree plantations	Smallholder agriculture
Outlet coordinates ^a	35°18'32.0472"E 0°27'47.592"S	35°13'17.22"E 0°28'34.9176"S	35°28'31.7316"E 0°24'4.0248"S
Area (km ²)	35.9	33.3	27.2
Elevation range (m a.s.l.)	1,968-2,385	1,788-2,141	2,389-2,691
Mean slope ± SD (%)	15.7±8.4	12.4±7.6	11.6±6.7
Basin order (Strahler)	2	2	2
Drainage density (km km ⁻²)	0.48	0.42	0.64
Soil infiltration rate (mm hr ⁻¹) ^b	760±500	430±290	401±211
Geology ^c	Igneous rock (Volcanic) (100%)	Igneous rock (Volcanic) (100%)	Igneous rock (Volcanic) (72%) & Pyroclastic (28%)
Dominant soils ^c	Humic Nitisols (100%)	Humic Nitisols (100%),	Humic Nitisols (72%) & mollic Andosols (28%)
Vegetation	Afromontane mixed forest, grassland, bamboo, broad- leafed evergreen trees and shrubs	Tea plantations with woodlots of <i>Eucalyptus</i> spp., <i>Cypress</i> spp. and <i>Pinus</i> spp.	Perennial & annual crops (maize interspersed with beans, potatoes, millet, cabbage and onions), woodlots, grassland
Riparian vegetation	Forest vegetation	>30 m buffer with indigenous vegetation	Degraded riparian vegetation, <i>Eucalyptus</i> woodlots

125 ^aWGS 1984 UTM Zone 36S

126 ^bOwuor et al. 2018

127 ^cKENSOTER Geology data from the Soil and Terrain database for Kenya (KENSOTER) version 2.0

128 The natural forest catchment is located in the South-West Mau block of the Mau Forest
129 Complex. The Mau Forest is an afromontane mixed forest dominated by indigenous broad-leafed
130 evergreen trees and shrubs with a complex vegetation pattern. Riparian forests with a mixture of
131 indigenous vegetation are present throughout the catchment. The natural forest catchment is
132 characterized by high infiltration rates with the occurrence of shallow to deeper subsurface water
133 pathways, whereas the tea-tree plantation and the smallholder agriculture catchments have lower
134 infiltration rates with a dominance of surface runoff (Jacobs *et al.* 2018a; Owuor *et al.* 2018)
135 (Table 1).

136 In the smallholder agriculture catchment, subsistence farmers grow maize interspersed with
137 beans, potatoes, millet and cabbage on small farms (circa 1 ha). Small-scale tea plantations,
138 eucalyptus (*Eucalyptus* spp.), cypress (*Cypressus* spp.) and pine (*Pinus* spp.) woodlots are
139 interspersed with crop fields and grazing land (Table 1). A combination of hand weeding, hoeing
140 and herbicides is used for weed control. Bamboo (*Bambusa* spp.) is generally found around
141 natural springs. The whole catchment is connected by a dense network of unpaved tracks either
142 bare or sparsely covered by grass; stream crossings rarely have bridges. The heavily travelled
143 unpaved tracks have commonly become eroded gullies (Figure 2a-b), that run down the slope to
144 rivers, connecting surface runoff from surrounding fields with the stream network (Figure 2c-e).
145 Cattle entrance points to the stream are generally highly disturbed and have degraded riverbanks
146 (Figure 2d-f). The natural riparian vegetation is in many areas replaced by Eucalyptus woodlots
147 or small bushes. In some places, riparian wetlands are found.



148
 149 Figure 2 a-c) Incised and unpaved tracks provide a direct connection with the stream, d-e) degraded and
 150 disturbed riverbank from livestock entering the streams and f) eroded suspended sediments in streams
 151 within the smallholder agriculture catchment.

152 The tea-tree plantation catchment has tea fields alternated with *Eucalyptus* spp. and *Cypress* spp.
 153 woodlots that are used for fuelwood at the tea factories. Some of the tea companies use mulch
 154 and rows of oat grass between rows of tea to control soil erosion during the establishment of new
 155 tea bushes. Herbicides are commonly used to control weeds. Cover crops with mature tea trees
 156 during the establishment of a new tea crop, terracing and sited cut-off drains are also used within
 157 the catchment to control soil erosion. The catchment is covered by a network of well-maintained
 158 paved and unpaved roads, linked to drainage systems, such as open culverts along the roads that
 159 connect them to the streams. The riparian vegetation includes a mix of indigenous tree species
 160 that cover densely the ground and form a buffer of approximately 30 m (Table 1).

161 The study area is composed of folded volcanics from the early Miocene times. Porphyritic
 162 phonolites, a member of the sequence of basic and intermediate lavas (igneous rocks) are

163 predominant in the study area (Binge 1962), where pyroclastic rocks cover the upper part of the
164 catchment (ISRIC 2007). The study area comprises well-drained, very deep (>1.8 m) dark-red
165 and dark-brown loamy soils (Sombroek *et al.* 1982), with moderate to high amounts of organic
166 matter under the forest cover (Dunne 1979).

167 2.2 Automated hydrological and sediment monitoring

168 This study uses a four year dataset (January 2015 to December 2018) on rainfall, discharge and
169 turbidity with a 10 minute resolution (Figure 1). A radar sensor (VEGAPULS WL61, VEGA
170 Grieshaber KG, Schiltach, Germany) collected continuous water level measurements. Water
171 level ('stage') was used to determine stream discharge based on a site-specific second-order
172 polynomial stage-discharge relationship (Jacobs *et al.* 2018b). The calibration was checked over
173 a wide range of stream flows using salt-dilution gauging (Shaw *et al.* 2011), an Acoustic
174 Doppler Velocimeter (ADV; FlowTracker, SonTek, San Diego CA, USA) or an Acoustic
175 Doppler Current Profiler (ADCP; RiverSurveyor S5, SonTek, San Diego, USA) depending on
176 river size and discharge (Jacobs *et al.* 2018b). Specific discharge [mm day^{-1}] was determined by
177 integrating instantaneous discharge taken at 10 minute intervals over a day and relating it to the
178 catchment area. Precipitation was measured using eight automatic tipping bucket rain gauges
179 calibrated to measure cumulative rainfall every 10 minutes with a 0.2 mm resolution (5 tipping
180 bucket rain gauges: Theodor Friedrichs, Schenefeld, Germany, and 3 weather stations: ECRN-
181 100 high resolution rain gauge). Using Thiessen polygons, we estimated the weighted
182 contribution of rainfall of every tipping bucket in each catchment. A more detailed description of
183 the study sites and instrumentation can be found in Jacobs *et al.* 2018b. Turbidity was measured
184 *in situ* as a surrogate for suspended sediment concentrations using a UV/Vis spectroscopy sensor
185 (spectro::lyser, s::can Messtechnik GmbH, Vienna, Austria). Turbidity is measured in FTU
186 (formazin turbidity unit) by transmitting a beam of light to an optical receptor. With an increase
187 in water turbidity the transmission of light decreases. To calculate sediment concentrations, a
188 site-specific turbidity-suspended sediment calibration was established (section 2.3.1). Before
189 each turbidity measurement, the window of the sensors was automatically cleaned by
190 compressed air to remove any interfering particles. The sensors were additionally cleaned
191 manually on a weekly basis using a specific cleaning agent recommended by the manufacturer to
192 reduce biofouling on the measurement window and by manually removing debris and sediment.

193 2.3 Calibration, quality assurance and analysis

194 2.3.1 Sediment-turbidity rating curve

195 We used a site-specific, *ex situ* incremental suspension calibration to convert long-term turbidity
196 records into an estimate of instantaneous suspended sediment concentrations (mg l^{-1}). A river
197 water-sediment suspension with 16 to 18 concentration increments was established to simulate
198 changing stream water suspended sediment concentrations occurring from low flow conditions
199 (minimum 0 mg l^{-1}) to storm events (maximum $4,607 \text{ mg l}^{-1}$). The sediment suspension consisted
200 of fine suspended sediment collected from sediment traps (time-integrated Phillips samplers) and
201 fine soil material mixed with turbid river water collected during storm events. To ensure that
202 only the clay size fraction remained in the suspension, the sediment suspension was decanted
203 twice after the settling time for coarse particles (particle size $>2 \mu\text{m}$) had elapsed (Stokes law:
204 98 sec). The spectro::lyser probes from each monitoring station measured each concentration
205 increment starting with river water representing low flow conditions (0 to 8 FTU). Small
206 quantities of the synthetic sediment suspension were added at each concentration increment until
207 the maximum measurable turbidity of 1,500 FTU was reached. The exact concentration was then
208 determined gravimetrically from a 250 ml sub-sample at each increment. Total suspended
209 sediment load was determined by multiplying suspended sediment concentration by discharge.
210 Suspended sediment yield was calculated by integrating the sediment load over time and relating
211 it to the catchment area. The sediment mass is reported in tonnes (t=megagrams) to conform with
212 other published values.

213 2.3.2 Data quality assurance

214 Quality assurance of the turbidity, discharge and precipitation dataset was performed in two
 215 different ways. First, during equipment maintenance and manually downloading of the data any
 216 observed anomalies were recorded in a log book. Potential causes of anomalous values included
 217 (i) sensor above water level, (ii) turbidity sensor completely buried by deposited sediment during
 218 storm periods, (iii) biofilm or other phenomena on the measurement window due to
 219 malfunctioning of automatic cleaning with compressed air, (iv) measurement gaps due to
 220 incidents of power supply failure or (v) counting of number of tips by the rain gauges restricted
 221 by blocked funnel or spiderwebs. The readings for these periods were flagged with
 222 Not-a-Number (NaN).

223 After anomalous values were replaced by NaN, the median absolute deviation (MAD) was used
 224 to detect local outliers. The MAD has the following form:

$$225 \quad MAD_i = b M_{i2}(|x_i - M_{i1}(x_i)|) \quad (1)$$

226 where x_i is the whole dataset, M_{i1} is the median of the dataset and M_{i2} is the median of the
 227 absolute deviation from the dataset from its median. The constant b estimates the standard
 228 deviation and was set to 1.4826 for normal distribution (Leys *et al.* 2013).

229 A moving window of k measurements around observation x_i at time t_i was used to detect local
 230 outliers with $x_j = (x_{i-k/2} \dots x_{i-1}, x_{i+1} \dots x_{i+k/2})$:

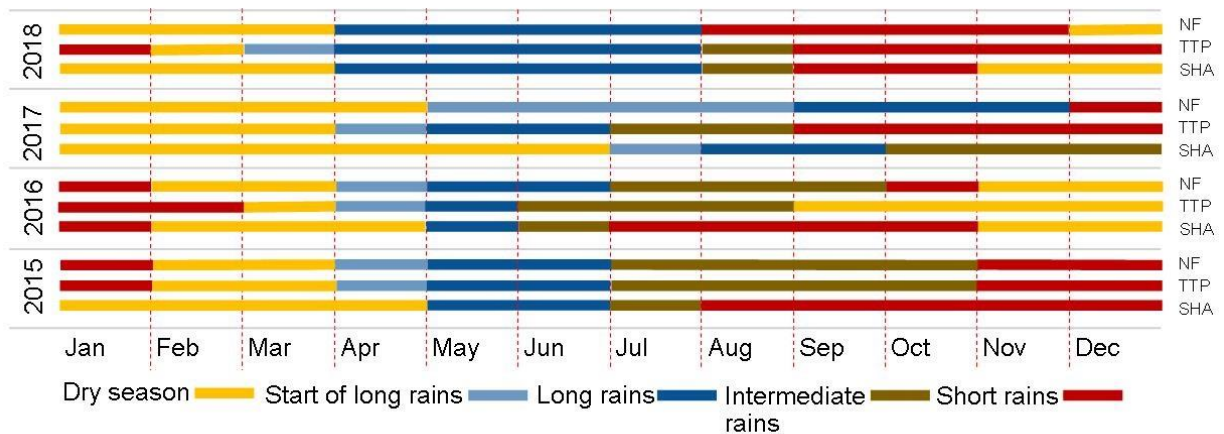
$$231 \quad \frac{x_i - M_{j,i}}{MAD_{j,i}} > a \quad (2)$$

232 where $a=6$ is the threshold for outlier selection, $M_{j,i}$ is the median and the $MAD_{j,i}$ is the MAD for
 233 x_j , while the moving window k was set to 16. Missing sediment data was interpolated using a
 234 linear function.

235 2.3.3 Data analysis

236 All data were tested for normality with the Shapiro-Wilk test. We tested significant differences
 237 on suspended sediment, rainfall and discharge values among the different land uses using
 238 Kruskal-Wallis test for analyses of variances. To detect the significance of the effect of land use
 239 on the hydrological and sedimentological parameters, and within and among seasons on
 240 suspended sediment load we used the pairwise Wilcoxon rank sum test.

241 Five seasons, dry season, start of long rains, long rains (long rainy season), intermediate rains
 242 (season between the long and short rainy season) and short rains (short rainy season), were
 243 identified to calculate their contribution to annual suspended sediment yield (Jacobs *et al.*
 244 2018b). The periods were chosen based on exceeding a threshold of monthly specific discharge
 245 for each catchment. The seasons for each year vary in length and timing due to variations in the
 246 onset of the rains and monthly streamflow (Figure 3).



247
 248 Figure 3 Timing of the five hydrological seasons for the natural forest (NF), tea-tree plantation (TTP) and
 249 smallholder agriculture (SHA) catchment during the observation period January 2015-December 2018.

250 2.3.4 Modelling flow pathways

251 A linear continuous-time (CT) transfer function (TF) model with rainfall-runoff non-linearity
 252 was used to identify the dynamics that explain the response of water flow pathways to rainfall
 253 within a catchment by conceptualising a *Single-Input, Single-Output* (SISO) system (Young &
 254 Garnier, 2006). These types of models are equivalent to systems of linear differential equations
 255 and can be applied in numerous mass and energy transport as well as chemical or biochemical
 256 process applications, including flow and sediment delivery models (Chappell *et al.* 2006). The

257 transfer function modelling process follows the *Data-Based Mechanistic* (DBM) modelling
 258 philosophy, searching through a range of model structures, ordering them according to statistical
 259 criteria, then retaining models that have a physical explanation (Young & Beven 1994). The
 260 DBM approach produces parsimonious models describing rainfall-runoff relationships, that
 261 include very few tuneable parameters (Lees 2000). Hourly time series of rainfall [mm hr⁻¹] was
 262 used as input, and the corresponding hourly time series of discharge [m³ sec⁻¹] as output (the
 263 units conversion is absorbed into the model coefficients, in case of Eq. 6 – into coefficient b_0).
 264 These parameters have hydrological interpretation, describing hydrological pathways, so while
 265 these are not strictly hydrological models derived from the process models, they still apply to
 266 hydrological systems (Beven 2012).

267 Hydrological processes are known to be non-linear (Beven 2012), with the effectiveness of
 268 rainfall (amount of rainfall converted into discharge) dependent upon the state of saturation of
 269 the catchment. Therefore, the rainfall-runoff non-linearity is modelled using the Hammerstein
 270 model structure, with the input (rainfall) transformed using a non-linear function into what is
 271 termed ‘effective rainfall’, which then drives the linear dynamics of the transport process model.
 272 This study uses a power law relationship between measured rainfall and effective rainfall as
 273 surrogate for soil moisture to translate rainfall to effective rainfall (See text S1 for more details).
 274 Effective rainfall is the dynamically changing proportion of rainfall representing the volume of
 275 streamflow generated after soil moisture storage is deducted from the total rainfall (Beven 2012).
 276 The RIVCBJ (Refined Instrumental Variable Continuous Time Box-Jenkins Identification, for
 277 continuous models, Young and Garnier, 2006) algorithm was used to estimate model parameters.
 278 RIVCBJ is a component of the CAPTAIN toolbox which runs within MATLAB[®] (Taylor *et al.*
 279 2007). The linear CT transfer function model has the following form:

$$280 \quad Y(s) = \frac{B(s)}{A(s)} U(s) e^{-s\tau} + E(s) \quad (3)$$

281 $A(s)$ and $B(s)$ characterise the dynamic relationship between the input and the output signals in
 282 the Laplace operator domain. The Laplace operator is the Laplace frequency domain equivalent
 283 of the time derivative operator $s \sim \frac{d}{dt}$. Functions $A(s)$ and $B(s)$ are constructed as polynomials in
 284 the s domain as follows, with m and n being the respective orders of the numerator and
 285 denominator polynomials:

286
$$A(s) = s^n + a_1s^{n-1} + \dots + a_ns^0 \quad (4)$$

287

288
$$B(s) = b_0s^{m-1} + b_1s^{m-2} + \dots + b_ms^0 \quad (5)$$

289 In Eq. (3) $Y(s)$ denotes the Laplace transform of the output signal as hourly streamflow
 290 [$\text{m}^3 \text{sec}^{-1}$], $U(s)$ is the Laplace transform of the input signal hourly rainfall [mm hr^{-1}], $E(s)$ are
 291 the model residuals and $e^{-s\tau}$ is the Laplace transform of time delay τ representing the pure time
 292 delay (as opposed to the dynamic lag resulting from the system's dynamics) in time units
 293 between the input and output signals.

294 In this study, up to third order models were tested for all the sites and model fit was evaluated
 295 according to the coefficient of determination (R_t^2) (also known as the Nash-Sutcliffe efficiency)
 296 (see text S2) and the Young Identification Criterion (YIC) (see text S3 and S4). First order
 297 transfer function models were selected for the three catchments, where each system has a
 298 different depletion time, determined by its time constant. A first order continuous time transfer
 299 function model is written as:

300
$$Y = \left(\frac{b_0}{s+a_1} \right) e^{-s\tau} U = \left(\frac{SSG}{STC+1} \right) e^{-s\tau} U \quad (6)$$

301 where $1/a_1$ is the time constant and the parameter b_0/a_1 represent the Steady State Gain (SSG)
 302 of the hypothetical pathway of rainfall through the catchment with a and b as the dynamic
 303 response characteristics. The time constant (TC) reflects the response between the input (rainfall)
 304 and the output (runoff or streamflow) (Young & Garnier 2006). Linear CT transfer function
 305 models were identified for each year between 2015 and 2018 for all three catchments.

306 2.3.5 Sediment response to hydrological variables

307 We used the cross-correlation function (CCF) to identify the statistical correlation between two
 308 sets of time series at different time lags (Lee *et al.* 2006; Mayaud *et al.* 2014). Rainfall and
 309 discharge time series were cross-correlated with the suspended sediment concentration time
 310 series. The peak response time between either precipitation or discharge to sediment
 311 concentrations was calculated as the delay time in time lags together with its correlation strength
 312 between these variables. Cross-correlation functions were calculated as:

$$313 \quad CCC(\tau) = \frac{\frac{1}{n} \sum (x_i - \bar{x})(y_{i-\tau} - \bar{y})}{\sigma_x \sigma_y} \quad (7)$$

314 where $CCC(\tau)$ is the cross-correlation coefficient at time lag τ , $\tau = 0, \pm 1 \pm 2 \dots \pm m$ between
 315 the two time series (sampled every 10 minutes), where x_i is observed rainfall or positive
 316 derivative of discharge at sample number i and $y_{i-\tau}$ is the suspended sediment concentration at
 317 sample number $i - \tau$, \bar{x} is the mean rainfall or positive derivative of discharge, \bar{y} is the mean
 318 suspended sediment concentration, σ_x is the standard deviation of rainfall or estimated positive
 319 derivative of discharge and σ_y is the standard deviation of suspended sediment and n is the
 320 number of data points. At the 95%-confidence interval, lag-time correlations are significant when
 321 $CCC(\tau)$ exceeds the standard error of $2/\sqrt{N}$, where N is the length of the dataset (Diggle 1990).
 322 The positive derivative of discharge, i.e. the estimated rate of change on the rising limb of the
 323 hydrograph, was selected because the main sediment pulses are mostly generated during the
 324 rising limb (Alexandrov *et al.* 2003; De Girolamo *et al.* 2015). A similar derivative effect has
 325 been observed in dynamic sediment load models by Walsh *et al.* (2011). The CCF analysis was
 326 carried out for each year between 2015 and 2018 for all three catchments.

327 **3 Results**

328 3.1 Hydrological response of the three catchments

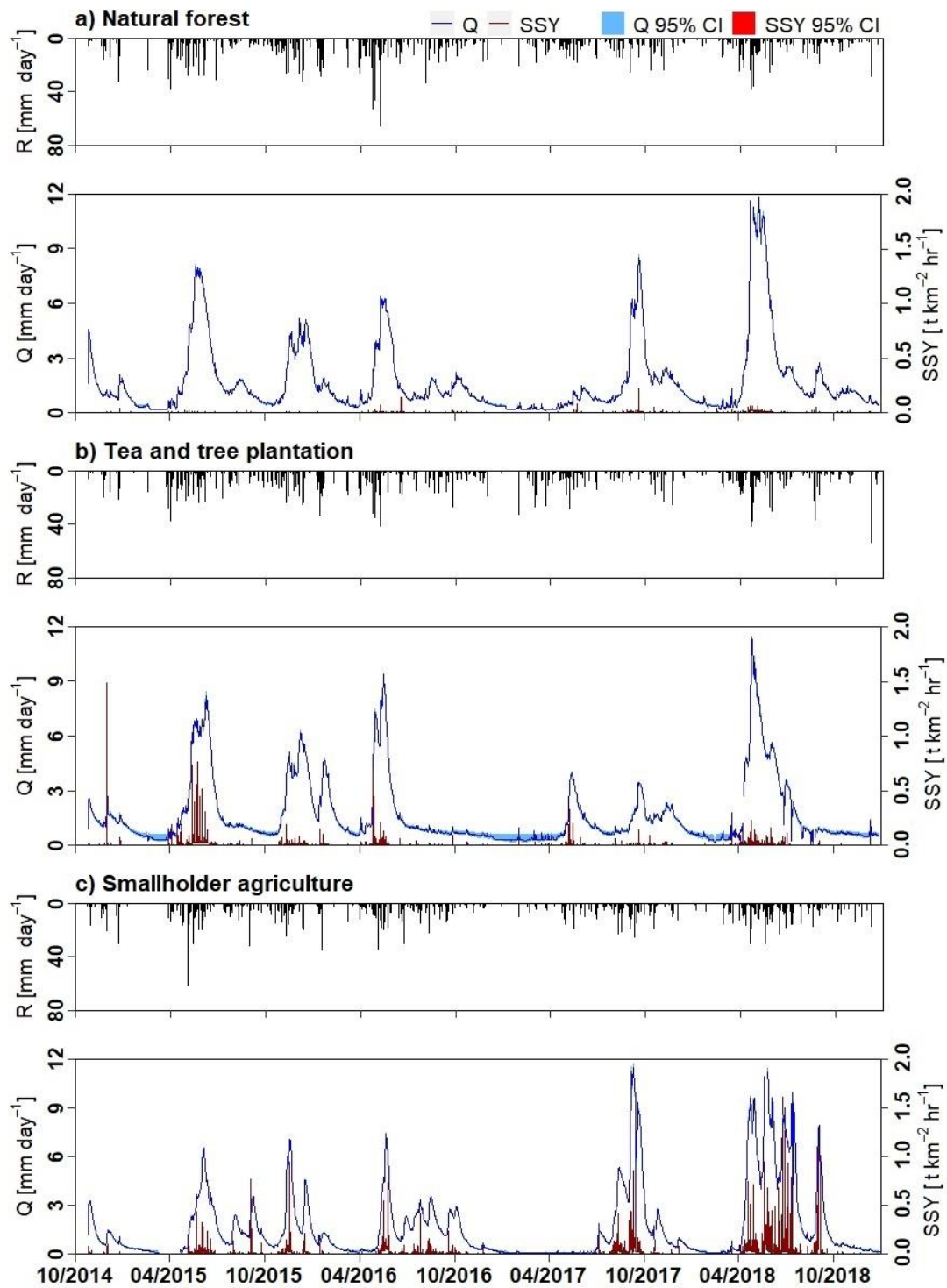
329 Mean annual rainfall for the study period was 1,842, 1,730 and 1,554 mm yr⁻¹ with maximum
 330 hourly rainfall over the whole observation period of 37.4, 33.1 and 27.5 mm hr⁻¹ for the natural
 331 forest, tea-tree plantations and smallholder agriculture catchments, respectively. The wettest year
 332 for the smallholder agriculture catchment was 2018 with 1,823 mm yr⁻¹ of rainfall, while for the
 333 natural forest and tea-tree plantations precipitation was highest in 2015 with 1,986 and
 334 1,928 mm yr⁻¹, respectively. The annual mean specific discharge was 632±157, 610±153 and
 335 621±224 mm yr⁻¹ for the natural forest, tea-tree plantations and smallholder agriculture
 336 catchments, respectively. The catchment runoff coefficient was similar for the natural forest and
 337 the tea-tree plantations with a mean of 0.34 and 0.35, respectively, and 0.39 for the smallholder
 338 agriculture (Table 2).

339 Table 2 Hydrological characteristics and total suspended sediment (and 95%-confidence interval) for the
 340 three catchments under different land use natural forest (NF; 35.9 km²), tea-tree plantations (TTP;
 341 33.3 km²) and smallholder agriculture (SHA; 35.9 km²) in the South-West Mau, Kenya. Different capital
 342 letters indicate significant differences between the different land uses (p<0.05).

Site	Year	Annual rainfall (mm yr ⁻¹)	Annual specific discharge (mm yr ⁻¹)	Runoff coefficient ^a	Total suspended sediment load (t yr ⁻¹)	Total suspended sediment yield (t km ⁻² yr ⁻¹)
NF	2015	1,986	714 (693-738)	0.36 (0.35-0.37)	407 (378-439)	11.3 (10.5-12.2)
	2016	1,846	518 (497-542)	0.28 (0.27-0.29)	667 (615-724)	18.6 (17.1-20.2)
	2017	1,783	483 (466-502)	0.27 (0.26-0.28)	673 (622-729)	18.7 (17.3-20.3)
	2018	1,755	812 (783-844)	0.46 (0.45-0.48)	1,337 (1,228-1,457)	37.2 (34.2-40.6)
Mean		1,842 A	632 (610-656) A	0.34 (0.33-0.36) A	771 (711-837) A	21.5 (19.8-23.2) A
TTP	2015	1,928	768 (730-820)	0.40 (0.38-0.43)	2,376 (2,185-2,603)	71.4 (65.6-78.2)
	2016	1,655	593 (555-642)	0.36 (0.34-0.39)	1,397 (1,277-1,539)	42.0 (38.4-46.2)
	2017	1,478	408 (372-468)	0.28 (0.25-0.32)	780 (701-880)	23.4 (21.0-26.4)
	2018	1,858	673 (634-728)	0.36 (0.34-0.39)	1,042 (952-1,151)	31.3 (28.6-34.5)
Mean		1,730 A	610 (573-665) A	0.35 (0.33-0.38) A	1,399 (1,279-1,543) A	42.0 (38.4-46.3) A
SHA	2015	1,607	561 (539-582)	0.35 (0.34-0.36)	2,324 (2,161-2,494)	85.4 (79.5-91.7)
	2016	1,369	479 (456-503)	0.35 (0.33-0.37)	2,271 (2,088-2,464)	83.5 (76.8-90.6)
	2017	1,416	492 (471-514)	0.35 (0.33-0.36)	2,440 (2,237-2,653)	89.7 (82.2-97.5)
	2018	1,823	953 (920-986)	0.52 (0.50-0.54)	7,273 (6,774-7,790)	267.4 (249.1-286.4)
Mean		1,554 A	621 (596-646) A	0.39 (0.38-0.41) A	3,577 (3,315-3,851) A	131.5 (121.9-141.6) B

343 ^aAnnual specific discharge as proportion of annual rainfall

344 Discharge in all catchments was flashy and varied seasonally. Rising limbs were generally steep
 345 and had variable falling limbs depending on event size. The highest discharge peaks were
 346 measured during the long rainy seasons between April and July in 2015, 2016 and 2018. In
 347 contrast, 2017 was the driest year with a late onset of the rains and the highest discharge peaks
 348 between August and November for the smallholder agriculture and the natural forest catchments.
 349 However, in the tea-tree plantation catchment the rains started in May lasting until November
 350 2017, resulting in discharge peaking in May and September 2017. High discharges were also
 351 recorded in January 2016 because the 2015 rains continued through November and December
 352 and were followed by an unusually wet January (Figure 4).

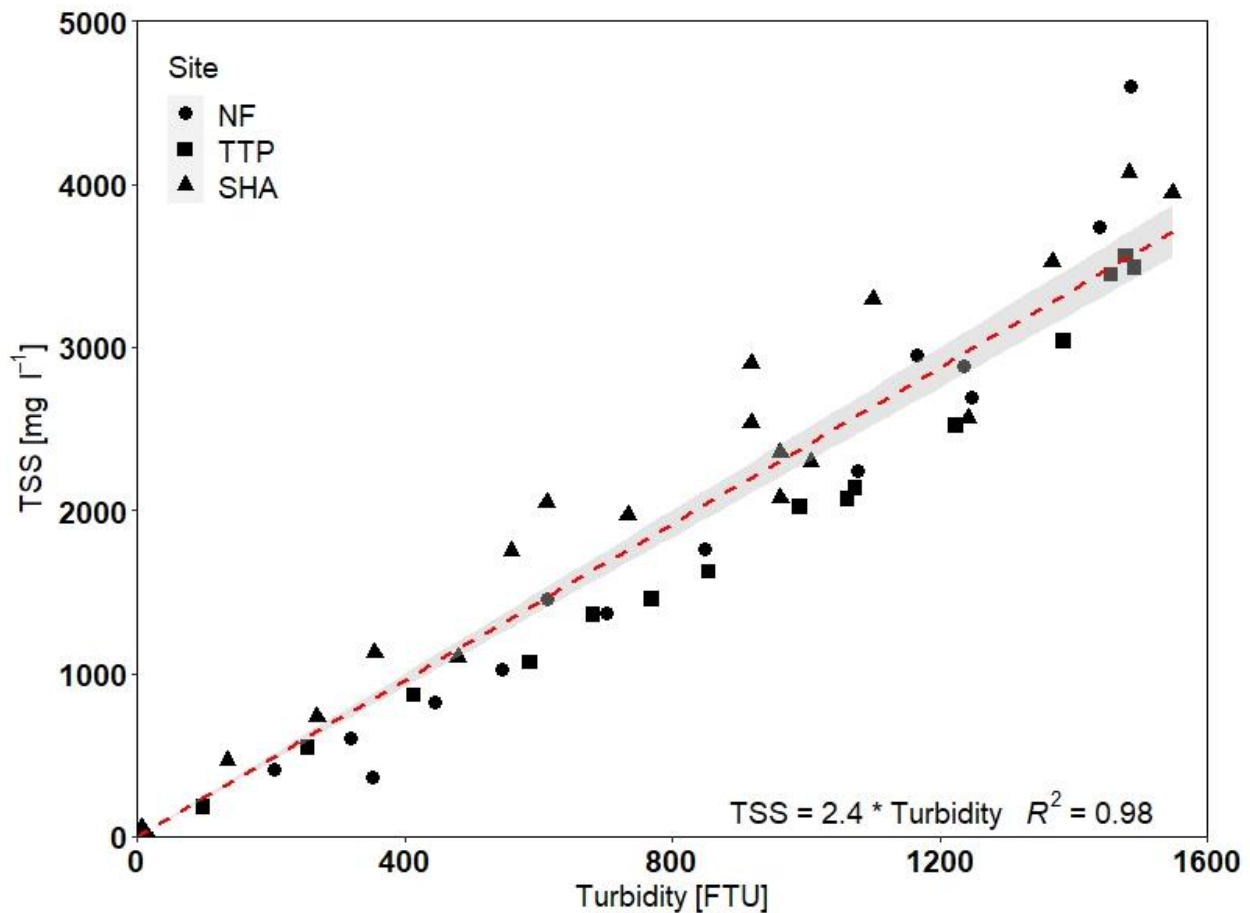


353

354 Figure 4 Time series of daily accumulated rainfall (R) [mm day⁻¹], daily specific discharge (Q)
 355 [mm day⁻¹] and hourly suspended sediment yield (SSY) [t km⁻² hr⁻¹] aggregated from 10 minute resolution
 356 with 95%-confidence interval of the a) natural forest, b) smallholder agriculture and c) tea-tree plantation
 357 catchments in the South-West Mau, Kenya, between October 2014 and December 2018.

358 3.2 Relationship between turbidity and suspended sediment concentration

359 We obtained one rating curve for all three catchments to predict suspended sediment
 360 concentration from the measured turbidity values. A linear model provided the best fit between
 361 the *in situ* turbidity and suspended sediment concentrations, and there was no significant
 362 difference between slopes for each site-specific calibration ($p\text{-value} > 0.1$). The intercept of the
 363 linear model was forced through the origin to prevent negative sediment concentrations at low
 364 turbidity, yielding an equation of the form $\text{TSS} = 2.4 * \text{turbidity}$ ($R^2 = 0.98$, $p\text{-value} < 0.001$, $n = 50$;
 365 Figure 5). This equation was used to convert the turbidity data to suspended sediment
 366 concentrations.



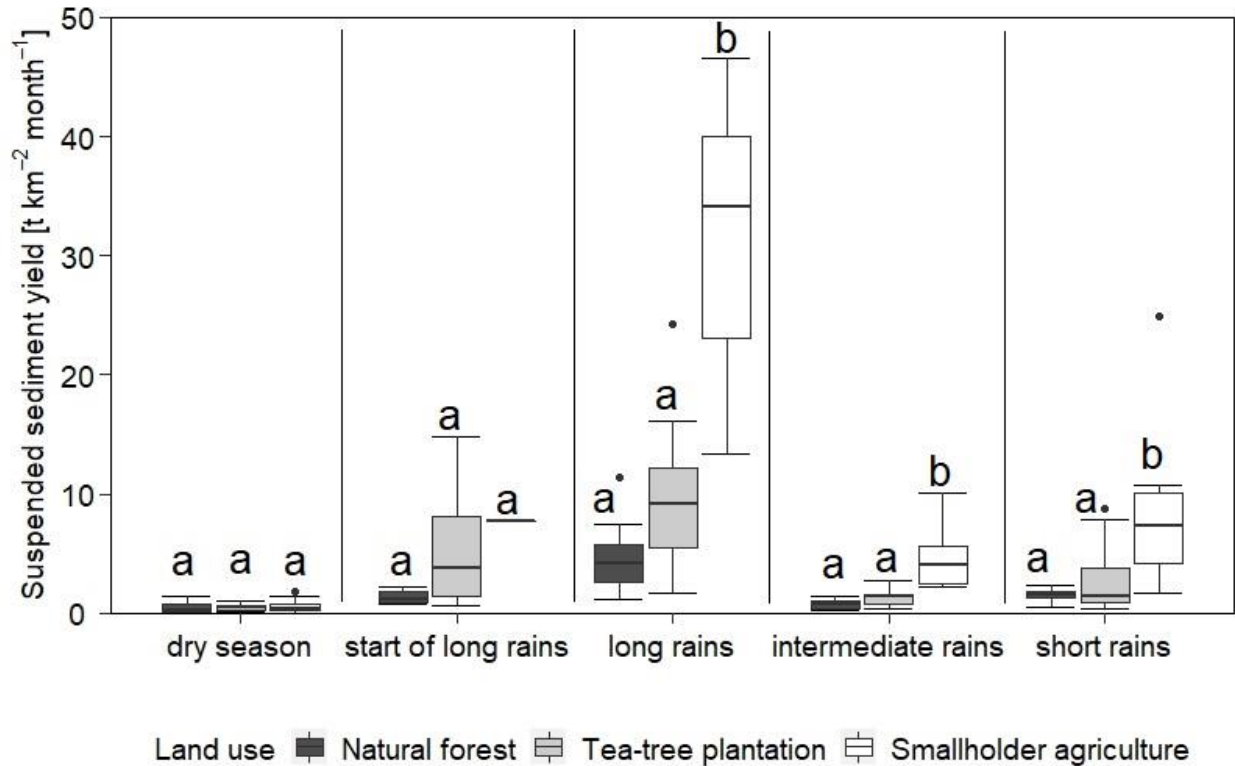
367
 368 Figure 5 Relation between total suspended sediment concentrations (TSS) [mg l^{-1}] and turbidity
 369 [FTU=Formazin Turbidity Unit] measurements for three catchments: natural forest (NF), tea-tree
 370 plantations (TTP) and smallholder agriculture (SHA) and the fitted linear model (grey shaded area:
 371 95%-confidence interval).

372 3.3 Suspended sediment dynamics

373 Sediment yield for the natural forest was lower than for the other two catchments (Figure 4). The
374 sedigraph of the natural forest had smaller peaks with a short event time, whereas the
375 smallholder agriculture and tea-tree plantations showed a steep increase followed by a flat
376 recession with a long event time. The sedigraph of the smallholder agriculture catchment showed
377 a flashy sediment response to rainfall and increased discharge. The maximum sediment yield in
378 the natural forest catchment was $0.2 \text{ t km}^{-2} \text{ hr}^{-1}$, followed by the tea-tree plantations with
379 $1.5 \text{ t km}^{-2} \text{ hr}^{-1}$ and the smallholder agriculture with a maximum sediment peak of $1.6 \text{ t km}^{-2} \text{ hr}^{-1}$
380 (Figure 4). The mean annual suspended sediment yield was significantly higher for the
381 smallholder agriculture catchment ($131.5 \pm 90.6 \text{ t km}^{-2} \text{ yr}^{-1}$) than for the tea-tree plantations
382 ($42.0 \pm 21.0 \text{ t km}^{-2} \text{ yr}^{-1}$) and the natural forest ($21.5 \pm 11.1 \text{ t km}^{-2} \text{ yr}^{-1}$) ($p < 0.05$) (Table 2). The
383 lowest mean suspended sediment concentration ($33.8 \pm 73.8 \text{ mg l}^{-1}$) was also lowest for the
384 natural forest catchment, followed by the tea-tree plantations ($47.4 \pm 90.7 \text{ mg l}^{-1}$). Concentrations
385 were three to four times higher at the outlet of the smallholder agriculture catchment
386 ($128.6 \pm 233.4 \text{ mg l}^{-1}$) than at the other catchments ($p = 0.04$). The daily mean suspended sediment
387 load from the natural forest was the lowest, followed by the tea-tree plantations and the
388 smallholder agriculture (2.1 , 3.9 and 10.0 t day^{-1} , respectively). The total suspended sediment
389 load for the entire study period (2015-2018) for the smallholder agriculture ($14,308 \text{ t}$) was four
390 times higher than that of the natural forest ($3,083 \text{ t}$), whereas sediment load for the tea-tree
391 plantations ($5,595 \text{ t}$) was only twice that of the natural forest. These loads represent a mean of
392 771 , $1,399$ and $3,577 \text{ t yr}^{-1}$ for the natural forest, tea-tree plantations and smallholder agriculture,
393 respectively. Suspended sediment yield increased from 2015 to 2018 in the natural forest and
394 smallholder agriculture catchments. In the tea-tree plantations, a similar sediment and rainfall
395 pattern was observed with a decline from 2015 to 2017 and then an increase again in 2018 (Table
396 2). The natural forest had the longest period of missing data lasting for 95 days in November
397 2015 to February 2016, followed by a shorter gap in the smallholder agriculture of 50 days from
398 March to April 2015 and the tea-tree plantations had the shortest period of missing sediment data
399 of 13 days between March and April 2017. Besides these periods, minor gaps were usually of
400 less than 24 hours with a total of missing sediment data of 7% for the natural forest, 2% for the
401 tea-tree plantations and 4% for the smallholder agriculture catchments between 2015-2018.

402 3.4 Seasonal variations in suspended sediment

403 During the study period, suspended sediment yield showed pronounced seasonal variability, with
404 most sediment being transported during the long rains in all catchments, and the highest monthly
405 yields being recorded for the smallholder agriculture catchment (Figure 6). Overall, more than
406 half of the sediment yield (45-52%) was attributed to the long rains, which cover less than one
407 third of the year. The sediment contribution during the long rains, intermediate rains and short
408 rains in the smallholder agriculture was significantly greater than in the natural forest and
409 tea-tree plantations ($p < 0.05$). For the natural forest the streams carried significantly more
410 material during the long rains (mean yield of $4.3 \pm 1.8 \text{ t km}^{-2} \text{ month}^{-1}$) than during any other
411 season. In the tea-tree plantations and smallholder agriculture, the sediment yield for the long
412 rains (mean 10.9 ± 6.9 and $30.7 \pm 10.6 \text{ t km}^{-2} \text{ month}^{-1}$, respectively) differed significantly from the
413 dry season (mean 0.4 ± 0.2 and $0.6 \pm 0.3 \text{ t km}^{-2} \text{ month}^{-1}$, respectively), the intermediate rains (mean
414 1.1 ± 0.6 and $5.4 \pm 3.3 \text{ t km}^{-2} \text{ month}^{-1}$, respectively) and the short rains (mean 3.2 ± 2.2 and
415 $23.9 \pm 26.1 \text{ t km}^{-2} \text{ month}^{-1}$, respectively), while there was no difference between the sediment
416 yield for the start of the long rains (mean 5.7 ± 6.5 and $7.8 \text{ t km}^{-2} \text{ month}^{-1}$, respectively) and the
417 long rains ($p < 0.05$).



418
 419 Figure 6 Boxplots of the monthly total suspended sediment yield [t km⁻² month⁻¹] for different seasons for
 420 the natural forest (NF), tea-tree plantations (TTPs) and smallholder agriculture (SHA) catchments in the
 421 South-West Mau, Kenya. Seasons: dry season, start of the long rainy season, long rainy season,
 422 intermediate rainy season and short rainy season between January 2015 and December 2018. Different
 423 letters above the box plot indicate significant differences between the land uses within each season
 424 ($p < 0.05$).

425 3.5 Flow pathways and streamflow dynamics

426 We compared hydrological flow pathways for each catchment as these are key in delivering
 427 sediments to the streams. Rainfall-runoff response was modelled over a continuous period of one
 428 year for each monitoring year 2015-2018 (see figure S1). In all three catchments, first order
 429 linear models (Eq. 6) were selected because these had the highest coefficients of determination
 430 (R_f^2) ranging between 86 and 93% and explained the data with the most negative YIC ranging
 431 between -12.5 and -10.4. The tea-tree plantations had a lower model performance in 2017
 432 compared to the other years with a R_f^2 value of 54% and a YIC of -8.3, where the first order
 433 model was identified as the optimal model (Table 3). A simple first order model was used to
 434 derive the time constant to compare the dynamic relationship between rainfall and runoff
 435 response among the three catchments. Our interpretation of the continuous time transfer function

436 model suggests a slower rainfall-runoff catchment response in the natural forest and tea-tree
 437 plantation catchments in contrast to the fast flow response to rainfall in the smallholder
 438 agriculture catchment. The time constants calculated ranged from 8.4 to 11.5 days in the natural
 439 forest catchment and from 9.6 to 13.0 days in the tea-tree plantations. The smallholder
 440 agriculture had time constants between 6.2 to 8.6 days (Table 3).

441 Table 3 Summary of the linear continuous-time transfer function models for the natural forest, tea-tree
 442 plantation and smallholder agriculture catchment in the South-West Mau, Kenya for four years (study
 443 period 2015-2018). YIC=Young Identification Criterion, R_t^2 =coefficient of determination, model
 444 structure [n =denominator polynomial, m =numerator polynomial, τ =pure time delay].

Site	Year	Time constant [days]	YIC	R_t^2	Model structure [n, m, τ]
Natural forest	2015	11.5	-11.2	0.92	[1 1 2]
	2016	12.6	-11.1	0.92	[1 1 2]
	2017	8.4	-11.2	0.92	[1 1 2]
	2018	9.8	-12.1	0.93	[1 1 2]
Tea-tree plantations	2015	12.1	-10.4	0.86	[1 1 2]
	2016	9.6	-11.5	0.90	[1 1 2]
	2017	13.0	-8.3	0.54	[1 1 2]
	2018	10.5	-11.4	0.92	[1 1 2]
Smallholder agriculture	2015 ^a	8.6	-10.7	0.86	[1 1 2]
	2016	8.7	-11.3	0.88	[1 1 3]
	2017	6.2	-12.5	0.96	[1 1 2]
	2018	6.9	-11.4	0.92	[1 1 2]

445 ^aData used in the analysis 1May-31Dec2015

446 3.6 Time lags between rainfall and discharge to sediment concentrations

447 The analysis using cross-correlation functions (CCF) (Eq. 7) showed statistically significant
 448 correlations between rainfall and discharge to suspended sediment exceeding the
 449 95%-confidence interval of 0.001 for a sample size of 61,201 in all three catchments for the four
 450 years. The CCF indicates the impulse response time between the peak of rainfall and discharge to
 451 the suspended sediment peak (see figure S2). The natural forest had almost instantaneous
 452 (<10 minutes) to rapid responses (1.5 hrs) in suspended sediment to both rainfall and discharge
 453 in all four years. A period shorter than a year was used for the natural forest in 2015 and 2016
 454 because of missing sediment data (Table 4). The rainfall to sediment cross-correlogram in the
 455 tea-tree plantations differed from the other two catchments, with a first fast peak within one hour
 456 followed by a delayed second peak after 5 to 8.5 hours. The discharge to sediment response in
 457 the tea-tree plantations was similar to that of the smallholder agriculture catchment with a time

458 lag of around two to three hours. The smallholder agriculture had variable time lags between
 459 either rainfall or discharge to sediment ranging between 1.5 to 3.8 hours. The impulse response
 460 time between the peaks of discharge and sediment concentration was in general longer compared
 461 to the rainfall peak (Table 4).

462 Table 4 Summary of cross-correlation functions (CCF) between rainfall/ positive derivative of discharge
 463 to suspended sediment with time lag (in hours) and peak cross-correlation coefficients reported for the
 464 natural forest, tea-tree plantation and smallholder agriculture catchment in the South-West Mau, Kenya
 465 over four years (study period 2015-2018).

Site	Year	Discharge to sediment		Rainfall to sediment	
		Time lag [hours]	CCF coefficient	Time lag [hours]	CCF coefficient
Natural forest	2015 ^a	1.0	0.10	1.5	0.16
	2016 ^a	<0.2	0.03	<0.2	0.05
	2017	0.5	0.07	<0.2	0.12
	2018	0.5	0.10	0.2	0.03
Tea-tree plantations ^b	2015	2.5	0.34	1 st 0.5 and 2 nd 6.5	1 st 0.08 and 2 nd 0.17
	2016	2.3	0.18	1 st 1.0 and 2 nd 7.0	1 st 0.08 and 2 nd 0.16
	2017	3.2	0.32	1 st 0.8 and 2 nd 8.5	1 st 0.08 and 2 nd 0.14
	2018	1 st 0.5 and 2 nd 2.0	1 st 0.17 and 2 nd 0.17	1 st 0.3 and 2 nd 5.0	1 st 0.18 and 2 nd 0.15
Smallholder agriculture	2015	2.8	0.27	0.7	0.13
	2016	2.2	0.18	1.5	0.08
	2017	3.8	0.17	1.5	0.11
	2018	2.2	0.21	3.5	0.15

466 ^aData used in the analysis 1Jan-22Nov2015 and 1Mar-31Dec2016

467 ^b1st and 2nd: identifies the first and second time lag and CCF coefficient of the CCF in the tea-tree plantations

468 **4 Discussion**

469 4.1 Suspended sediment dynamics

470 This study shows that the annual suspended sediment yield is around six times greater for the
 471 drier smallholder agriculture catchment, and twice greater in the tea-tree plantation catchment
 472 compared to the wetter natural forest catchment. The sediment yield difference is likely the result
 473 of more vegetation cover and low surface hydrological connectivity in the natural forest, where
 474 consequently erosion processes (including mass wasting) are not as active. Similar findings were
 475 reported for the neighbouring Mara river basin, where a semi-arid catchment had higher
 476 suspended sediment yields ($44 \text{ t km}^{-2} \text{ yr}^{-1}$) with half of the annual rainfall in contrast to a wetter,

477 but less populated and less disturbed catchment ($33 \text{ t km}^{-2} \text{ yr}^{-1}$) (Dutton et al., 2018) (**Fehler!**
478 **Verweisquelle konnte nicht gefunden werden.**)

479

480 Table 5 Overview of different studies reporting annual suspended sediment yields (SSY) in Kenyan headwater streams and tropical montane forest
 481 catchments worldwide derived from gauging station measurements.

Montane catchment	Area (km ²)	Land use	Study period (year)	Annual rainfall (mm yr ⁻¹)	SSY (t km ⁻² yr ⁻¹)	Reference
Sub-catchments of Sondu basin (West Kenya)	35.9	Natural forest	2014-2018	1,842	21	This study
	33.3	Tea-tree (<i>Eucalyptus</i>) plantations	2014-2018	1,730	42	
	27.2	Smallholder agriculture	2014-2018	1,554	131	
Different catchments throughout southern half of Kenya	n.a.	Natural forest (100%)	1948-1968	n.a.	20-30	Dunne, 1979
	n.a.	Natural forest (>51%)	1948-1968	n.a.	10-100	
	n.a.	Agricultural land (>50%)	1948-1968	n.a.	10-1,500	
	n.a.	Grazing land	1948-1968	n.a.	5,000-20,000	
Athi (Kenya)	510	Agriculture, grazing land and settlements	1985	n.a.	109	Kithiia, 1997
Upper Mara-Emarti (South-West Kenya)	2,450	Smallholder agriculture and urban development	2011-2014 (3-4 months)	1,400	33	Dutton et al., 2018
		Grazing land	2011-2014 (3-4 months)	600	44	Dutton et al., 2018
Middle Mara-Talek (South-West Kenya)						
Ruharo (Uganda)	2,121	Grazing land, agriculture, <20% Papyrus wetlands	2009-2010	1,535	106	Ryken et al., 2015
Koga (Uganda)	379	Grazing land, agriculture, >80% Papyrus wetlands	2009-2010	1,330	37	Ryken et al., 2015
Andit Tid (Ethiopia)	4.77	Agriculture (30%)	1989-1996	1,467	522	Guzman et al., 2013
Anjeni (Ethiopia)	1.13	Agriculture (80%)	1989-1996	1,675	2,470	
Maybar (Ethiopia)	1.12	Agriculture (60%)	1989-2001	1,417	740	Nyssen et al., 2009
May Zegzeg (Ethiopia)	1.87	Agriculture and grazing land	2000	774	850	
		Agriculture and grazing land with soil conservation practices	2006	708	190	
Arvorezinha (South Brazil)	1.23	Agriculture with traditional soil management & natural forest	2002-2003	2,051	298	Minella et al., 2018
		Agriculture with soil conservation practices & natural forest	2004-2008	1,655	68	
		Agriculture with traditional soil management & cultivated forest	2009-2016	2,102	163	
Conceição (South Brazil)	800	>85% agriculture (soybean, wheat, oats, ryegrass) with soil management, <15% gallery forest, wetlands and urban areas	2000-2010	1718	140	Didoné et al., 2014
			2011	1,422	242	
			2012	1,463	41	
Guaporé (South Brazil)	2,000	Agriculture (soybean, tobacco, maize, oats, ryegrass), grazing land and cultivated forest	2000-2010	1550	140	Didoné et al., 2014
			2011	1,195	390	
			2012	1,660	158	
Baru (Borneo)	0.44	Disturbed logged natural forest	1989	3,205	1,632	Douglas et al., 1993
		Natural forest immediately after logging	1991	2,609	1,017	
		Natural forest after logging	1995-1996	2,956	592	
W8S5 (Borneo)	1.7	Natural forest	1989	3,205	118	Douglas et al., 1993
			1991	2,609	117	
			2006-2008	1,743	323	
Mae Sa (Thailand)	74.2	Natural forest (62%) and agriculture (>20%)	2006-2008	1,743	323	Ziegler et al., 2014
Basper (Philippines)	0.32	Grassland and shrubs	2013	2,660	2,740	Zhang et al., 2018

n.a.=no data available

482
483

484 Missing sediment data and linear interpolation to fill these gaps could have increased the
485 uncertainty in the sediment yields calculated. However, data gaps during dry periods, such as
486 those in the sediment data for the natural forest during 2015 and 2016, would not have a large
487 influence on yield calculations because of the small amount of material transported. Gaps during
488 periods of heavy rainfall, which occasionally occurred in the smallholder agriculture catchment
489 due to siltation, could have contributed to underestimation of the sediment yield, as peaks in the
490 sediment concentration could be missing.

491 For Africa, suspended sediment yield was estimated to be $634 \text{ t km}^{-2} \text{ yr}^{-1}$ at continental scale
492 based on 682 catchments and rivers with larger drainage areas (mean $>1,000 \text{ km}^2$) (Vanmaercke
493 *et al.* 2014). Compared to this, and other sediment studies in Kenya with varying catchment sizes
494 of $24\text{-}42,000 \text{ km}^2$ and 8.2 to $6,330 \text{ t km}^{-2} \text{ yr}^{-1}$ (Dunne, 1979; Vanmaercke *et al.*, 2014), our
495 annual suspended sediment yields ($21\text{-}131 \text{ t km}^{-2} \text{ yr}^{-1}$) are within the lower reported ranges.
496 Suspended sediment yields from the tea-tree plantations and natural forest catchment of our
497 study are comparable to those observed in the neighbouring upper Mara river basin
498 ($33 \text{ t km}^{-2} \text{ yr}^{-1}$; Dutton *et al.*, 2018), which is dominated by small-scale farming and urban
499 development. The smallholder agriculture catchment in our study had slightly higher suspended
500 sediment yields than the Athi catchment in Kenya ($109 \text{ t km}^{-2} \text{ yr}^{-1}$; Kithiia, 1997) and had lower
501 suspended sediment yields than disturbed agricultural catchments in montane headwaters such as
502 the May Zegzeg catchment in Ethiopia ($850 \text{ t km}^{-2} \text{ yr}^{-1}$; Nyssen *et al.*, 2009) or the Arvorezinha,
503 Conceição and Guapore catchments in South Brazil ($140\text{-}298 \text{ t km}^{-2} \text{ yr}^{-1}$; Didoné *et al.*, 2014;
504 Minella *et al.*, 2018). Guzman *et al.* (2013) found that in Ethiopia the highest suspended
505 sediment yields ($2,470 \text{ t km}^{-2} \text{ yr}^{-1}$) in small catchments were in those with the largest proportion
506 of agricultural land. Their reported annual yields were significantly higher than the suspended
507 sediment yields observed in this study with similar annual rainfall. Annual suspended sediment
508 yields of 117 up to $2,740 \text{ t km}^{-2} \text{ yr}^{-1}$ from undisturbed to highly disturbed forest or upland
509 grassland catchments were measured in South-East Asia (Borneo, Thailand and the Philippines)
510 subjected to mass wasting during typhoon or post-typhoon events.

511 4.2 Factors controlling sediment yield

512 *Vegetation cover*

513 The low annual suspended sediment yield measured in the Mau forest shows that forest
514 vegetation is the most effective surface cover to limit soil erosion despite the steepest slopes of
515 the forested catchment (Table 1). The dense vegetation, diverse strata and complex rooting
516 systems prevent soil detachment and trap potentially erodible material. Similarly, a dense
517 perennial tea vegetation covers the soil surface in the tea-tree plantations, which can buffer
518 erosive rainfall (Edwards & Blackie 1979). Nevertheless, the annual suspended sediment yield
519 for the tea-tree plantation catchment was twice that of the natural forest despite the soil
520 conservation practices applied by tea companies such as mulching, planting of buffer strips (oat
521 grass) between rows of young tea bushes or cover trees on newly planted tea plots. This indicates
522 that high sediment loads originate from unprotected bare surfaces during renovation of tea
523 plantations or logging activities of woodlots. Logging activities trigger overland flow and
524 erosion processes and lead sediments to the streams, when there are no buffer strips (Douglas *et*
525 *al.* 1993; Chappell *et al.* 2004). The dense vegetation contrasts with the land management in the
526 smallholder agriculture catchment, where steep slopes tend to be bare between crop harvest and
527 the start of the next cropping season. During that period, bare surfaces are prone to soil erosion,
528 although cropland surface erosion was not observed, which may be explained by the high
529 infiltration rates previously measured on these croplands ($401 \pm 211 \text{ mm hr}^{-1}$) (Owuor *et al.*
530 2018). The routing of main flow paths was observed on compacted gullied tracks which act as
531 ephemeral channels during a storm event. Based on these observations, we hypothesize that rural
532 unpaved tracks in the smallholder agriculture generate a larger contribution to the total sediment
533 load than agricultural land, but further work is required to confirm this. A potential reason for the
534 annual increase in suspended sediment yield in the smallholder agriculture and the natural forest
535 catchments during the study period could be the reduced tree cover and increasing areas under
536 annual crops and forest disturbance indicated by the study of Brandt *et al.* (2018).

537 *Connectivity between sediment sources and the streams*

538 The tea-tree plantations and the smallholder agriculture have higher catchment surface
539 connectivity than the natural forest, which may be causing higher sediment transfer by
540 connecting multiple source areas with the streams. Lateral linkages (tracks, gullies or drains)
541 connect sediment source areas at catchment-scale with the stream network (Lane & Richards
542 1997), which can be an important driving force for the total sediment load into the rivers (Sidle

543 & Ziegler 2010).

544 In the smallholder agriculture catchment, unpaved tracks are the main pathways for people and
545 livestock to access streams, thus being frequently used and heavily trafficked also by motorbikes
546 (Figure 2). This activity generates highly compacted surfaces, where soil infiltration is impeded.
547 Ziegler et al. (2001) observed that unpaved rural roads, similar in appearance to the unpaved
548 tracks of our study, generate significantly more overland flow compared to adjacent hillslopes.
549 As a consequence of low infiltration rates and downslope-orientated tracks, surface runoff
550 energy increases generating more volume and velocity of flow that can transport large quantities
551 of soil, eventually eroding tracks into gullies (Svoray & Markovitch 2009; Sidle & Ziegler
552 2010). Other researchers found a strong influence of subsurface water tables in valleys on gully
553 formation and the development of large scale sediment mobilization (Tebebu *et al.* 2010; Zegeye
554 *et al.* 2018). High sediment loads at the outlet of the smallholder agriculture catchment are
555 thought to originate from the eroded unpaved tracks and its connecting adjacent source areas.
556 Catchment drainage density is higher in the smallholder agriculture (0.64 km km^{-2}) compared to
557 the natural forest and tea-tree plantations (0.48 and 0.42 km km^{-2} , respectively) suggesting a link
558 to increased erosion rates. The tea-tree plantation catchment is hydrologically connected through
559 a network of tracks and well-engineered paved and unpaved drains in between the tea fields. The
560 design of the well-engineered drains took into account the appropriate routing of surface runoff
561 to the riparian zones before entering the streams, suggesting a higher hydrological connectivity
562 than in the smallholder agriculture catchment. However, the drains are well-maintained with a
563 densely forested riparian zone, which reduces sediment export, thereby reducing sediment
564 transport connectivity. The strong hydrological connectivity of the tea-tree plantation catchment
565 could lead to high sediment transport and loads with poor maintenance of the drainage network.

566 *Riparian zones*

567 Dense riparian vegetation can trap sediments before they reach the stream (Pavanelli & Cavazza
568 2010). An intact forested riparian zone in the natural forest and a riparian buffer of 30 m, as pre-
569 described by the Kenya's Water Act (Republic of Kenya 2012), of mixed indigenous vegetation
570 in the tea-tree plantations seem to be reducing sediment delivery to the streams by trapping
571 eroded soil. In contrast, high sediment loads are expected in the smallholder agriculture

572 catchment, where the riparian vegetation is highly degraded or replaced by crops or woodlots
573 planted on the river banks. Small floodplains in a steep, narrow valley floor provide limited
574 space for sediment storage. In the same river basin, other studies reported that highly degraded
575 riparian zones adjacent to areas cultivated by smallholder agriculture lead to increased suspended
576 sediment concentrations (Masese *et al.* 2012; Njue *et al.* 2016). In the smallholder agriculture
577 catchment, livestock access the streams through the riparian area for watering (Figure 2d-f),
578 which damages the riverbank and the riparian vegetation and further increases sediment supply.

579 4.3 Water pathways are key for sediment production

580 Hydrological pathways such as surface runoff or subsurface flow are key in determining
581 sediment response in catchments. Our analysis showed that the natural forest and tea-tree
582 plantation catchments, with lower suspended sediment yields had the longest streamflow
583 response time to rainfall using the CT transfer function model (Eq. 6). This supports our
584 hypothesis that shorter pathways indicate that surface runoff mobilizes soil particles causing six
585 times more suspended sediment yields.

586 The number of pathways and their response time depend on catchment characteristics (Chappell
587 *et al.* 2006; Ockenden & Chappell 2011). Forest ecosystems are generally characterized by
588 complex catchment behaviour (Chappell *et al.* 1999), where soils with high infiltration rates
589 promote infiltration to deeper subsurfaces. These pathways can be divided into shallow water
590 pathway and deep groundwater pathway (Chappell & Franks 1996). The high infiltration rates
591 ($760 \pm 500 \text{ mm hr}^{-1}$, Owuor *et al.* 2018) and the long time constants derived through modelling for
592 the natural forest catchment (Table 3) point to subsurface flow pathways. Jacobs *et al.* (2018a)
593 reported the occurrence of shallow to deeper subsurface flow by using an endmember mixing
594 analysis in the same natural forest catchment. Groundwater seemed to be an important stream
595 water source (Jacobs *et al.*, 2018a), which agrees with the long response time we calculated
596 (Table 3). Our findings corroborate those of other studies in tropical forest catchments, which
597 demonstrated that subsurface flow is the main water pathway of forest ecosystems (Noguchi *et*
598 *al.* 1997; Boy *et al.* 2008; Muñoz-Villers & McDonnell 2013). Consequently, low suspended
599 sediment yields are associated with limited surface erosion and sediment delivery to the streams
600 in the natural forest catchment.

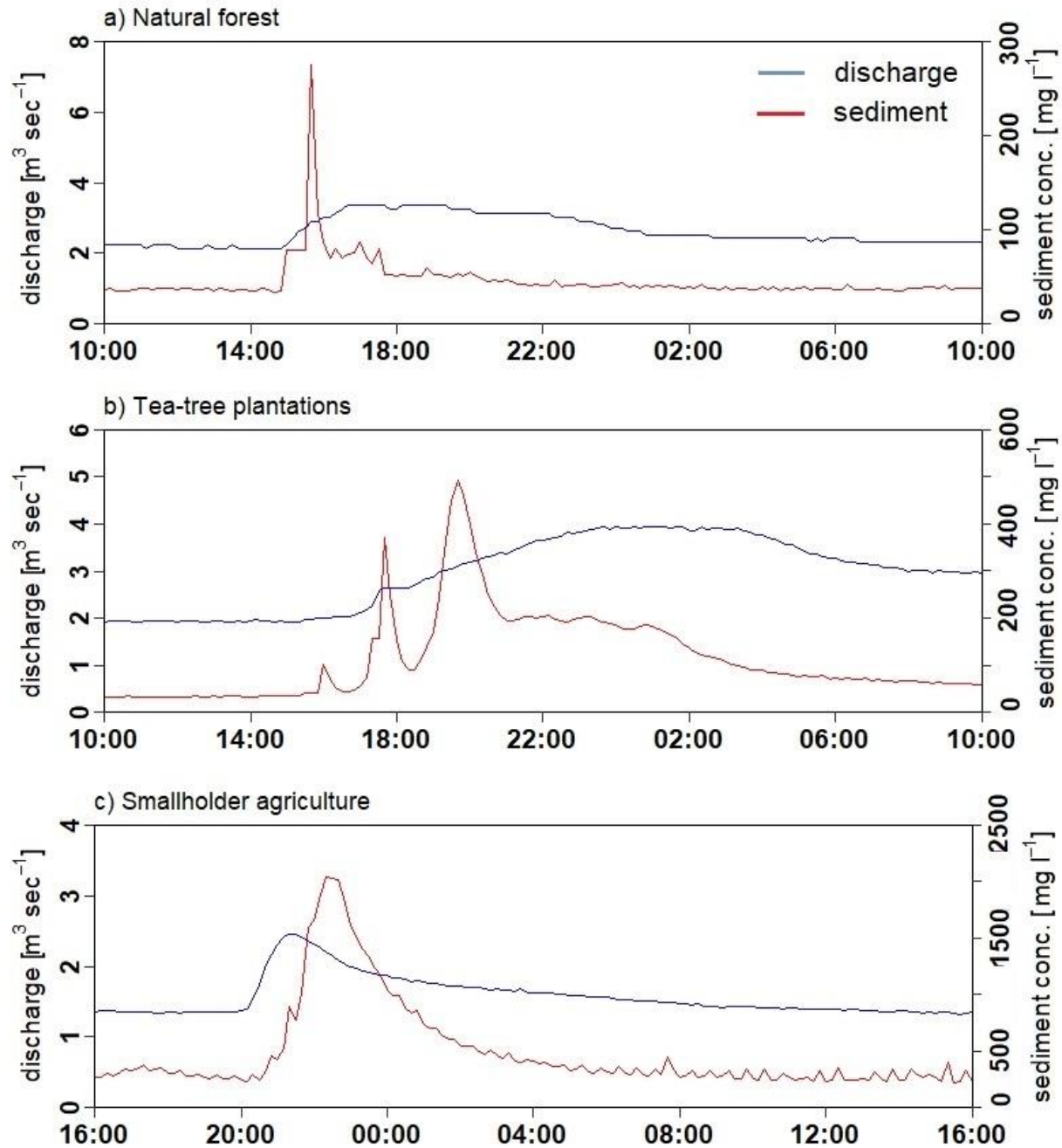
601 The main pathways in the tea-tree plantations with slightly shorter time constants (Table 3) and
602 almost half the infiltration rate (430 ± 290 mm hr⁻¹, Owuor *et al.* 2018) compared to the natural
603 forest suggest that shallow subsurface flow and surface runoff may dominate. Overland flow was
604 observed to be routed through the well-engineered drainage network along roads and surface
605 water drains between tea plantations to the well buffered fluvial network. Overland flow was
606 also thought to be significant by Jacobs *et al.* (2018b), where nitrate concentrations in stream
607 water seemed to be diluted by surface runoff. The well-maintained drains explain the lower
608 suspended sediment yields, despite the prevalence of surface runoff observed in the tea-tree
609 plantations.

610 The analysis of the smallholder agriculture catchment showed a relatively fast pathway.
611 However, Owuor *et al.* (2018) measured infiltration rates of 401 ± 211 mm hr⁻¹ on croplands in
612 the catchment, suggesting that subsurface flow is the most likely pathway. Nevertheless, field
613 observations of runoff along with poorly maintained highly compacted tracks, and the shape of a
614 classification of hysteresis loops by Jacobs *et al.* (2018b) provides a contrasting insight
615 suggesting that surface runoff in the smallholder agriculture is an important vector for sediment.
616 Our hypothesis is that the tracks act as ephemeral streams and receive water from the
617 surrounding areas as shallow lateral flow, thus explaining the shorter water response times. The
618 natural forest and tea-tree plantation catchment with high tree cover showed similar time
619 constants, whereas the much lower tree cover in the smallholder agriculture catchment lead to
620 faster pathways. The generally slow pathway component in each model can be explained by the
621 presence of deep and well-drained soils in all catchments (Sombroek *et al.* 1982).

622 4.4 Sediment response times and event duration

623 The shorter time lag between the peaks of rainfall to sediment than to discharge can be attributed
624 to exposed and easy erodible material adjacent to the outlet. The almost instantaneous sediment
625 response to rainfall in the natural forest and tea-tree plantations suggest sediment supply from
626 readily available, nearby sediment sources (Francke *et al.* 2014; Tena *et al.* 2014; De Girolamo
627 *et al.* 2015) (Figure 7). Near-channel or in-channel sediment sources can originate from the
628 stream bank or the stream bed (Kronvang *et al.* 1997; Chappell *et al.* 1999; Lenzi & Marchi
629 2000). Temporarily stored sediment is thought to be mobilized very quickly during the first
630 stages of a storm event (Eder *et al.* 2010). Fast response systems of short duration and low mass

631 magnitude, as those observed in the natural forest catchment, are characterized by rapid sediment
632 flushing and fast depletion of sediment supply (Chappell *et al.* 1999), due to limited availability
633 of eroded material from the protected surface (Fang *et al.* 2008; Fan *et al.* 2012; De Girolamo *et*
634 *al.* 2015). The paved drain network in the tea-tree plantation catchment can act as conduits
635 transporting sediment instantaneously from nearby logged plantations or tracks to the stream.
636 The delayed sediment response after a rainfall event in the smallholder agriculture and the
637 second sediment response in the tea-tree plantation catchment suggest a long travel distance
638 between the sediment source and the catchment outlet. The delayed response can be related to
639 the magnitude of mass, where more distant sediment source areas from the wider catchment
640 accumulate more mass over a longer period. These responses may also indicate the breaching of
641 barriers such as hedges, fences or grazing land, especially in the smallholder agriculture
642 catchment. The long recession limb in the smallholder agriculture and the tea-tree plantation
643 catchments is typically explained as a slow depletion of sediment supply (Francke *et al.* 2014;
644 Tena *et al.* 2014; De Girolamo *et al.* 2015). The more pronounced sedigraph in the smallholder
645 agriculture catchment can be associated with the wide range of accumulated sediment source
646 areas (Figure 7).



647
 648 Figure 7 Typical shape of the sedigraph (sediment conc.=concentration [mg l⁻¹] and hydrograph
 649 (discharge [m³ sec⁻¹] (10 minute resolution) for events in the natural forest (02/06-03/06/2018 10:00), the
 650 tea-tree plantation (24/04-25/04/2018 10:00) and the smallholder agriculture (17/05-18/05/2018 16:00)
 651 catchment in the South-West Mau, Kenya.

652 4.5 Seasonal variability of suspended sediment

653 Throughout the study period, we observed distinct seasonal variability in suspended sediment
654 yield for the natural forest, tea-tree plantations and smallholder agriculture with higher yields in
655 periods of high discharge and rainfall. In climates with strong seasonality of rainfall, seasons can
656 explain sediment dynamics (Horowitz 2008; De Girolamo *et al.* 2015), as we observed in this
657 study. Wet seasons or high-flow events generate the largest proportion (80-95%) of the annual
658 sediment load, as observed by De Girolamo *et al.* (2015), Sun *et al.* (2016) and Vercruysse *et al.*
659 (2017) in other areas, while the sediment load is the smallest in the dry season with less than 5%
660 in our study. The seasonal differences were more pronounced in the smallholder agriculture
661 catchment compared to the other two catchments explained by the high catchment surface
662 connectivity and low vegetation cover.

663 **5 Conclusions**

664 This study presents the first long-term high-resolution sediment dataset in Kenya. The four years
665 of continuous data for the natural forest, tea-tree plantation and smallholder agriculture
666 catchments provide critical insights in contrasting sediment dynamics of the tropical montane
667 Mau Forest Complex. The analysis revealed that land use is a critically important driver for
668 sediment supply, where smallholder agriculture generates six times more annual suspended
669 sediment yield than a catchment dominated by natural forest. Besides vegetation cover, a strong
670 catchment surface connectivity through unpaved tracks and gullies from hillslopes to the fluvial
671 network is thought to be the main reason for the differences in sediment yields. However, further
672 work is required to test this hypothesis. Catchments with a high tree cover, such as the natural
673 forest and the tea-tree plantations seem to have similar water pathways with a dominance of
674 subsurface flow. In contrast, in the highly disturbed landscape such as that of the smallholder
675 agriculture catchment, surface runoff dominates and soil erosion increases suspended sediment
676 yield. This superficial water pathway results in the more pronounced seasonal impact of rainfall
677 in the smallholder agriculture compared to the other two catchments, also due to varying
678 vegetation cover. Delayed sediment response to rainfall and a slow depletion in sediment supply
679 in the smallholder agriculture and tea-tree plantations suggests that the wider catchment area is
680 supplying sediment from a range of sediment sources, especially in the catchment dominated by

681 smallholder farming. In contrast, the fast depletion in sediment supply in the natural forest
682 suggests the importance of nearby sediment sources and temporarily stored sediment.

683 Land scarcity and population growth bring enormous pressure on natural forest ecosystems.
684 Forest conversion will increase sediment production, which will affect, not only many people in
685 the Sondu River basin who rely on the rivers for drinking water, but also Lake Victoria which is
686 already affected by increased sediment supply. The implementation of catchment management,
687 such as soil conservation measures and better engineering of rural trackways is essential to
688 reduce sediment supply to water bodies. However, a detailed sediment source fingerprinting
689 analysis is necessary to identify the main contributing sediment sources. This will support the
690 application of better management strategies at the source to prevent sediment entering the stream
691 network. Sediment yields reported in other sediment studies in montane smallholder agriculture
692 catchments were higher than in our study, which provide a warning of potentially higher
693 sediment loss in the future unless mitigation strategies are implemented.

694 **Acknowledgements**

695 We thank the German Federal Ministry for Economic Cooperation and Development (Grant
696 81206682 “The Water Towers of East Africa: policies and practices for enhancing co-benefits
697 from joint forest and water conservation”) and the Deutsche Forschungsgemeinschaft DFG
698 (Grant BR2238/23-1) for providing financial support for this research. This work was also
699 partially funded by the CGIAR program on Forest, Trees and Agroforestry led by the Centre for
700 International Forestry Research (CIFOR). We would like to thank the tea companies, the Kenya
701 Forest Service (KFS) and the chief of the smallholder agriculture catchment (Kuresoi sub-
702 location) for supporting our research activities, and Naomi K. Njue for maintenance of the
703 equipment. Finally, we are also grateful for the valuable and constructive comments from the
704 associate editor and three anonymous reviewers. The raw data are available online
705 (<https://dx.doi.org/10.17635/lancaster/researchdata/352>) hosted by Lancaster University, UK.

706 **References**

- 707 Alexandrov, Y., Laronne, J.B. & Reid, I. (2003). Suspended sediment concentration and its
708 variation with water discharge in a dryland ephemeral channel, northern Negev, Israel. *J.*
709 *Arid Environ.*, 53, 73–84.
- 710 Beven, K.J. (2012). *Rainfall-runoff modelling: The Primer*. Wiley-Blackwell, Chichester, UK.

- 711 Binge, F.W. (1962). Geology of the Kericho area, Ministry of commerce, Industry and
712 Communications, Geological Survey of Kenya, 2–73.
- 713 Boy, J., Valarezo, C. & Wilcke, W. (2008). Water flow paths in soil control element exports in
714 an Andean tropical montane forest. *Eur. J. Soil Sci.*, 59, 1209–1227.
- 715 Brandt, P., Hamunyela, E., Herold, M., de Bruin, S., Verbesselt, J. & Rufino, M.C. (2018).
716 Sustainable intensification of dairy production can reduce forest disturbance in Kenyan
717 montane forests. *Agric. Ecosyst. Environ.*, 265, 307–319.
- 718 Brown, T., Schneider, H. & Harper, D. (1996). Multi-scale estimates of erosion and sediment
719 yields in the Upper Tana basin, Kenya. In: *Erosion and Sediment Yield: Global and*
720 *regional perspectives*. IAHS Publ, Exeter, pp. 49–54.
- 721 Bruijnzeel, L.A. (2004). Hydrological functions of tropical forests: not seeing the soil for the
722 trees? *Agric. Ecosyst. Environ.*, 104, 185–228.
- 723 Chappell, N.A., Douglas, I., Hanapi, J.M. & Tych, W. (2004). Sources of suspended sediment
724 within a tropical catchment recovering from selective logging. *Hydrol. Process.*, 18, 685–
725 701.
- 726 Chappell, N.A. & Franks, S. (1996). Property distributions and flow structure in the Slapton
727 Wood Catchment. *F. Stud.*, 8, 698–718.
- 728 Chappell, N.A., McKenna, P., Bidin, K., Douglas, I. & Walsh, R.P.D. (1999). Parsimonious
729 modelling of water and suspended sediment flux from nested catchments affected by
730 selective tropical forestry. *Philos. Trans. R. Soc. London. Ser. B Biol. Sci.*, 354, 1831–1846.
- 731 Chappell, N.A., Tych, W., Chotai, A., Bidin, K., Sinun, W. & Chiew, T.H. (2006).
732 BARUMODEL: Combined Data Based Mechanistic models of runoff response in a
733 managed rainforest catchment. *For. Ecol. Manage.*, 224, 58–80.
- 734 Didoné, E.J., Minella, J.P.G., Reichert, J.M., Merten, G.H., Dalbianco, L., de Barros, C.A.P., *et*
735 *al.* (2014). Impact of no-tillage agricultural systems on sediment yield in two large
736 catchments in Southern Brazil. *J. Soils Sediments*, 14, 1287–1297.
- 737 Diggle, P. (1990). *Time series: a biostatistical introduction*. 5th edn. Clarendon Press, Oxford,
738 UK.
- 739 Douglas, I., Greer, T., Bidin, K. & Sinun, W. (1993). Impact of roads and compacted ground on
740 post-logging sediment yield in a small drainage basin, Sabah, Malaysia. In: *Hydrology of*
741 *Warm Humid Regions*. IAHS Publ, Yokohama Symposium, pp. 213–218.
- 742 Dunne, T. (1979). Sediment yield and land use in tropical catchments. *J. Hydrol.*, 42, 281–300.
- 743 Dutton, C.L., Subalusky, A.L., Anisfeld, S.C., Njoroge, L., Rosi, E.J. & Post, D.M. (2018). The
744 influence of a semi-arid sub-catchment on suspended sediments in the Mara River, Kenya.
745 *PLoS One*, 13, 1–19.
- 746 Eder, A., Strauss, P., Krueger, T. & Quinton, J.N. (2010). Comparative calculation of suspended
747 sediment loads with respect to hysteresis effects (in the Petzenkirchen catchment, Austria).
748 *J. Hydrol.*, 389, 168–176.
- 749 Edwards, K.A. & Blackie, J.R. (1979). The Kericho research project. *East African Agric. For. J.*,
750 43, 44–50.

- 751 Fan, X., Shi, C., Zhou, Y. & Shao, W. (2012). Sediment rating curves in the Ningxia-Inner
752 Mongolia reaches of the upper Yellow River and their implications. *Quat. Int.*, 282, 152–
753 162.
- 754 Fang, H., Chen, H., Cai, Q. & Huang, X. (2008). Effect of spatial scale on suspended sediment
755 concentration in flood season in hilly loess region on the Loess Plateau in China. *Environ.*
756 *Geol.*, 54, 1261–1269.
- 757 Foster, I.D.L., Rowntree, K.M., Boardman, J. & Mighall, T.M. (2012). Changing sediment yield
758 and sediment dynamics in the Karoo Uplands, South Africa; Post-European Impacts. *L.*
759 *Degrad. Dev.*, 23, 508–522.
- 760 Foy, R.H. & Bailey-Watts, A.E. (1998). Observations on the spatial and temporal variation in the
761 phosphorus status of lakes in the British Isles. *Soil Use Manag.*, 14, 131–138.
- 762 Francke, T., Werb, S., Sommerer, E. & López-Tarazón, J.A. (2014). Analysis of runoff, sediment
763 dynamics and sediment yield of subcatchments in the highly erodible Isábena catchment,
764 Central Pyrenees. *J. Soils Sediments*, 14, 1909–1920.
- 765 Fraser, A.I., Harrod, T.R. & Haygarth, P.M. (1999). The effect of rainfall intensity on soil
766 erosion and particulate phosphorus transfer from arable soils. *Water Sci. Technol.*, 39, 41–
767 45.
- 768 Fryirs, K. (2013). (Dis)Connectivity in catchment sediment cascades: a fresh look at the
769 sediment delivery problem. *Earth Surf. Process. Landforms*, 38, 30–46.
- 770 Gellis, A.C. & Mukundan, R. (2013). Watershed sediment source identification: tools,
771 approaches, and case studies. *J. Soils Sediments*, 13, 1655–1657.
- 772 De Girolamo, A.M., Pappagallo, G. & Lo Porto, A. (2015). Temporal variability of suspended
773 sediment transport and rating curves in a Mediterranean river basin: The Celone (SE Italy).
774 *CATENA*, 128, 135–143.
- 775 Githui, F., Gitau, W., Mutua, F. & Bauwens, W. (2009). Climate change impact on SWAT
776 simulated streamflow in western Kenya. *Int. J. Climatol.*, 29, 1823–1834.
- 777 Grangeon, T., Legout, C., Esteves, M., Gratiot, N. & Navratil, O. (2012). Variability of the
778 particle size of suspended sediment during highly concentrated flood events in a small
779 mountainous catchment. *J. Soils Sediments*, 12, 1549–1558.
- 780 Guzman, C.D., Tilahun, S.A., Zegeye, A.D. & Steenhuis, T.S. (2013). Suspended sediment
781 concentration–discharge relationships in the (sub-) humid Ethiopian highlands. *Hydrol.*
782 *Earth Syst. Sci.*, 17, 1067–1077.
- 783 Hilton, J., O’Hare, M., Bowes, M.J. & Jones, J.I. (2006). How green is my river? A new
784 paradigm of eutrophication in rivers. *Sci. Total Environ.*, 365, 66–83.
- 785 Horowitz, A.J. (2008). Determining annual suspended sediment and sediment-associated trace
786 element and nutrient fluxes. *Sci. Total Environ.*, 400, 315–343.
- 787 ISRIC. (2007). Soil and terrain database for Kenya (KENSOTER), version 2.0, at scale 1:1
788 million. Wageningen, The Netherlands: World Soil Information, 8–10.
- 789 Jacobs, S.R., Timbe, E., Weeser, B., Rufino, M.C., Butterbach-Bahl, K. & Breuer, L. (2018a).
790 Assessment of hydrological pathways in East African montane catchments under different

- 791 land use. *Hydrol. Earth Syst. Sci.*, 22, 4981–5000.
- 792 Jacobs, S.R., Weeser, B., Guzha, A.C., Rufino, M.C., Butterbach-Bahl, K., Windhorst, D., *et al.*
 793 (2018b). Using high-resolution data to assess land use impact on nitrate dynamics in East
 794 African tropical montane catchments. *Water Resour. Res.*, 54, 1812–1830.
- 795 Kemp, P., Sear, D., Collins, A., Naden, P. & Jones, I. (2011). The impacts of fine sediment on
 796 riverine fish. *Hydrol. Process.*, 25, 1800–1821.
- 797 Kithiia, M.S. (1997). Land use changes and their effects on sediment transport and soil erosion
 798 within the Athi drainage basin, Kenya. In: *Human impact on erosion and sedimentation.*
 799 *Proc. international symposium.* IAHS Publ, Rabat, Morocco, pp. 145–150.
- 800 Krhoda, G.O. (1988). The impact of resource utilization on the hydrology of the Mau Hills
 801 Forest in Kenya. *Mt. Res. Dev.*, 8, 193.
- 802 Kronvang, B., Laubel, A. & Grant, R. (1997). Suspended sediment and particulate phosphorus
 803 transport and delivery pathways in an arable catchment, Gelbæk stream, Denmark. *Hydrol.*
 804 *Process.*, 11, 627–642.
- 805 Lane, S.N. & Richards, K.S. (1997). Linking river channel form and process: time, space and
 806 causality revisited. *Earth Surf. Process. Landforms*, 22, 249–260.
- 807 Lee, L.J.E., Lawrence, D.S.L. & Price, M. (2006). Analysis of water-level response to rainfall
 808 and implications for recharge pathways in the Chalk aquifer, SE England. *J. Hydrol.*, 330,
 809 604–620.
- 810 Lees, M.J. (2000). Data-based mechanistic modelling and forecasting of hydrological systems. *J.*
 811 *Hydroinformatics*, 2, 15–34.
- 812 Lefrançois, J., Grimaldi, C., Gascuel-Oudou, C. & Gilliet, N. (2007). Suspended sediment and
 813 discharge relationships to identify bank degradation as a main sediment source on small
 814 agricultural catchments. *Hydrol. Process.*, 21, 2923–2933.
- 815 Lenzi, M.A. & Marchi, L. (2000). Suspended sediment load during floods in a small stream of
 816 the Dolomites (northeastern Italy). *CATENA*, 39, 267–282.
- 817 Lewis, J. (1996). Turbidity-controlled suspended sediment sampling for runoff-event load
 818 estimation. *Water Resour. Res.*, 32, 2299–2310.
- 819 Leys, C., Ley, C., Klein, O., Bernard, P. & Licata, L. (2013). Detecting outliers: Do not use
 820 standard deviation around the mean, use absolute deviation around the median. *J. Exp. Soc.*
 821 *Psychol.*, 49, 764–766.
- 822 Masese, F.O., Raburu, P.O., Mwasi, B.N. & Etiégni, L. (2012). Effects of deforestation on water
 823 resources: integrating science and community perspectives in the Sondu-Miriu River Basin,
 824 Kenya. *New Adv. Contrib. to For. Res. InTech*, 3–18.
- 825 Mayaud, C., Wagner, T., Benischke, R. & Birk, S. (2014). Single event time series analysis in a
 826 binary karst catchment evaluated using a groundwater model (Lurbach system, Austria). *J.*
 827 *Hydrol.*, 511, 628–639.
- 828 Minella, J.P.G., Clarke, R.T., Merten, G.H. & Walling, D.E. (2008). Sediment source
 829 fingerprinting: testing hypotheses about contributions from potential sediment sources. In:
 830 *Sediment dynamics in changing environments.* IAHS Publ, Christchurch, New Zealand, pp.

- 831 31–37.
- 832 Minella, J.P.G., Merten, G.H., Barros, C.A.P., Ramon, R., Schlesner, A., Clarke, R.T., *et al.*
833 (2018). Long-term sediment yield from a small catchment in southern Brazil affected by
834 land use and soil management changes. *Hydrol. Process.*, 32, 200–211.
- 835 Mogaka, H., Gichere, S., Davis, R. & Hirji, R. (2006). *Climate variability and water resources*
836 *degradation in Kenya: improving water resources development and management.* World
837 Bank, Washington, D.C.
- 838 Morgan, R.P.C. (2005). *Soil erosion and conservation.* 3rd edn. Blackwell Publishing Ltd,
839 Cranfield, UK.
- 840 Morris, G.L. (2014). Sediment management and sustainable use of reservoirs. In: *Modern Water*
841 *Resources Engineering.* Humana Press, Totowa, NJ, pp. 279–337.
- 842 Muñoz-Villers, L.E. & McDonnell, J.J. (2013). Land use change effects on runoff generation in a
843 humid tropical montane cloud forest region. *Hydrol. Earth Syst. Sci.*, 17, 3543–3560.
- 844 Njue, N., Koech, E., Hitimana, J. & Sirmah, P. (2016). Influence of land use activities on
845 riparian vegetation, soil and water quality: an indicator of biodiversity loss, south West Mau
846 forest, Kenya. *Open J. For.*, 06, 373–385.
- 847 Noguchi, S., Nik, A.R., Kasran, B., Tani, M., Sammori, T. & Morisada, K. (1997). Soil physical
848 properties and preferential flow pathways in tropical rain forest, Bukit Tarek, Peninsular
849 Malaysia. *J. For. Res.*, 2, 115–120.
- 850 Ntiba, M.J., Kudoja, W.M. & Mukasa, C.T. (2001). Management issues in the Lake Victoria
851 watershed. *Lakes Reserv. Res. Manag.*, 6, 211–216.
- 852 Nyssen, J., Clymans, W., Poesen, J., Vandecasteele, I., De Baets, S., Haregeweyn, N., *et al.*
853 (2009). How soil conservation affects the catchment sediment budget - a comprehensive
854 study in the north Ethiopian highlands. *Earth Surf. Process. Landforms*, 34, 1216–1233.
- 855 Nyssen, J., Poesen, J., Moeyersons, J., Deckers, J., Haile, M. & Lang, A. (2004). Human impact
856 on the environment in the Ethiopian and Eritrean highlands—a state of the art. *Earth-*
857 *Science Rev.*, 64, 273–320.
- 858 Ockenden, M.C. & Chappell, N.A. (2011). Identification of the dominant runoff pathways from
859 data-based mechanistic modelling of nested catchments in temperate UK. *J. Hydrol.*, 402,
860 71–79.
- 861 Ogden, F.L., Crouch, T.D., Stallard, R.F. & Hall, J.S. (2013). Effect of land cover and use on dry
862 season river runoff, runoff efficiency, and peak storm runoff in the seasonal tropics of
863 Central Panama. *Water Resour. Res.*, 49, 8443–8462.
- 864 Owens, P.N., Batalla, R.J., Collins, A.J., Gomez, B., Hicks, D.M., Horowitz, A.J., *et al.* (2005).
865 Fine-grained sediment in river systems: environmental significance and management issues.
866 *River Res. Appl.*, 21, 693–717.
- 867 Owuor, S.O., Butterbach-Bahl, K., Guzha, A.C., Jacobs, S., Merbold, L., Rufino, M.C., *et al.*
868 (2018). Conversion of natural forest results in a significant degradation of soil hydraulic
869 properties in the highlands of Kenya. *Soil Tillage Res.*, 176, 36–44.
- 870 Pavanelli, D. & Cavazza, C. (2010). River suspended sediment control through riparian

- 871 vegetation: a method to Detect the Functionality of Riparian Vegetation. *CLEAN - Soil, Air,*
872 *Water*, 38, 1039–1046.
- 873 Pellikka, P., Clark, B., Hurskainen, P., Keskinen, A., Lanne, M., Masalin, K., *et al.* (2004). Land
874 use change monitoring applying geographic information system in the Taita hills, SE-
875 Kenya. African association of Remote Sensing of Environmental, Nairobi, Kenya, p. 8.
- 876 Poesen, J., Nachtergaele, J., Verstraeten, G. & Valentin, C. (2003). Gully erosion and
877 environmental change: importance and research needs. *CATENA*, 50, 91–133.
- 878 Quinton, J.N., Catt, J.A. & Hess, T.M. (2001). The selective removal of phosphorus from soil. *J.*
879 *Environ. Qual.*, 30, 538.
- 880 Ramos-Scharrón, C.E. & Thomaz, E.L. (2016). Runoff development and soil erosion in a wet
881 tropical montane setting under coffee cultivation. *L. Degrad. Dev.*, 28, 936–945.
- 882 Republic of Kenya. (2012). *Water Act, laws of Kenya*. 2nd edn. National Council for Law
883 Reporting with the Authority of the Attorney-General, Nairobi, Kenya.
- 884 Ryken, N., Vanmaercke, M., Wanyama, J., Isabirye, M., Vanonckelen, S., Deckers, J., *et al.*
885 (2015). Impact of papyrus wetland encroachment on spatial and temporal variabilities of
886 stream flow and sediment export from wet tropical catchments. *Sci. Total Environ.*, 511,
887 756–766.
- 888 Shaw, E.M., Beven, K.J., Chappell, N.A. & Lamb, R. (2011). *Hydrology in practice*. 4th edn.
889 Taylor & Francis, London and New York.
- 890 Sidle, R.C. & Ziegler, A.D. (2010). Elephant trail runoff and sediment dynamics in northern
891 Thailand. *J. Environ. Qual.*, 39, 871.
- 892 Sombroek, W.G., Braun, H.M.H. & van der Pouw, B.J. (1982). *Exploratory soil map and agro-*
893 *climatic zone map of Kenya, 1980, scale 1:1,000,000*. E1 edn. Ministry of Agriculture -
894 National Agricultural Laboratories, Kenya.
- 895 Sun, L., Yan, M., Cai, Q. & Fang, H. (2016). Suspended sediment dynamics at different time
896 scales in the Loushui River, south-central China. *CATENA*, 136, 152–161.
- 897 Svoray, T. & Markovitch, H. (2009). Catchment scale analysis of the effect of topography,
898 tillage direction and unpaved roads on ephemeral gully incision. *Earth Surf. Process.*
899 *Landforms*, 34, 1970–1984.
- 900 Taylor, C.J., Pedregal, D.J., Young, P.C. & Tych, W. (2007). Environmental time series analysis
901 and forecasting with the Captain toolbox. *Environ. Model. Softw.*, 22, 797–814.
- 902 Tebebu, T.Y., Abiy, A.Z., Zegeye, A.D., Dahlke, H.E., Easton, Z.M., Tilahun, S.A., *et al.*
903 (2010). Surface and subsurface flow effect on permanent gully formation and upland
904 erosion near Lake Tana in the northern highlands of Ethiopia. *Hydrol. Earth Syst. Sci.*, 14,
905 2207–2217.
- 906 Tena, A., Vericat, D. & Batalla, R.J. (2014). Suspended sediment dynamics during flushing
907 flows in a large impounded river (the lower River Ebro). *J. Soils Sediments*, 14, 2057–2069.
- 908 Trimble, S.W. & Mendel, A.C. (1995). The cow as a geomorphic agent — A critical review.
909 *Geomorphology*, 13, 233–253.

- 910 UNEP, KWS & KFWG. (2005). Mau Complex under siege: Continuous destruction of Kenya's
911 largest forest. UNEP, Kenya.
- 912 USGS. (2000). *Shuttle Radar Topography Mission (SRTM) 1 Arc-Second Global*. U. S.
913 Geological Survey, Reston, Virginia, USA.
- 914 Vanmaercke, M., Poesen, J., Broeckx, J. & Nyssen, J. (2014). Sediment yield in Africa. *Earth-*
915 *Science Rev.*, 136, 350–368.
- 916 Vanmaercke, M., Zenebe, A., Poesen, J., Nyssen, J., Verstraeten, G. & Deckers, J. (2010).
917 Sediment dynamics and the role of flash floods in sediment export from medium-sized
918 catchments: a case study from the semi-arid tropical highlands in northern Ethiopia. *J. Soils*
919 *Sediments*, 10, 611–627.
- 920 Vercruyssen, K., Grabowski, R.C. & Rickson, R.J. (2017). Suspended sediment transport
921 dynamics in rivers: Multi-scale drivers of temporal variation. *Earth-Science Rev.*, 166, 38–
922 52.
- 923 Verschuren, D., Johnson, T.C., Kling, H.J., Edgington, D.N., Leavitt, R., Brown, E.T., *et al.*
924 (2002). History and timing of human impact on Lake Victoria, East Africa. *R. Soc.*, 269,
925 289–294.
- 926 Walling, D.E. & Webb, B.W. (1996). Erosion and sediment yield: a global overview. In: *Erosion*
927 *and Sediment Yield: Global and regional perspectives*. IAHS Publ, Exeter, p. 17.
- 928 Walsh, R.P.D., Bidin, K., Blake, W.H., Chappell, N.A., Clarke, M.A., Douglas, I., *et al.* (2011).
929 Long-term responses of rainforest erosional systems at different spatial scales to selective
930 logging and climatic change. *Philos. Trans. R. Soc. B Biol. Sci.*
- 931 Wangechi, K.S., Muigai, A.W.T. & Ouma, S.O. (2015). The impact of evolution and socio-
932 economics of commercially exploited fish stock: A review on *Rastrineobola argentea* in
933 Lake Victoria. *J. Food Secur.*, 3, 82–86.
- 934 Wohl, E. (2006). Human impacts to mountain streams. *Geomorphology*, 79, 217–248.
- 935 Young, P.C. & Beven, K.J. (1994). Data-based mechanistic modelling and the rainfall-flow non-
936 linearity. *Environmetrics*, 5, 335–363.
- 937 Young, P.C. & Garnier, H. (2006). Identification and estimation of continuous-time, data-based
938 mechanistic (DBM) models for environmental systems. *Environ. Model. Softw.*, 21, 1055–
939 1072.
- 940 Zegeye, A.D., Langendoen, E.J., Guzman, C.D., Dagnew, D.C., Amare, S.D., Tilahun, S.A., *et*
941 *al.* (2018). Gullies, a critical link in landscape soil loss: A case study in the subhumid
942 highlands of Ethiopia. *L. Degrad. Dev.*, 29, 1222–1232.
- 943 Zhang, J., van Meerveld, H.J. (Ilja.), Tripoli, R. & Bruijnzeel, L.A. (2018). Runoff response and
944 sediment yield of a landslide-affected fire-climax grassland micro-catchment (Leyte, the
945 Philippines) before and after passage of typhoon Haiyan. *J. Hydrol.*, 565, 524–537.
- 946 Ziegler, A.D., Benner, S.G., Tantasirin, C., Wood, S.H., Sutherland, R.A., Sidle, R.C., *et al.*
947 (2014). Turbidity-based sediment monitoring in northern Thailand: Hysteresis, variability,
948 and uncertainty. *J. Hydrol.*, 519, 2020–2039.
- 949 Ziegler, A.D., Giambelluca, T.W., Sutherland, R.A., Vana, T.T. & Nullet, M.A. (2001). Horton

950 overland flow contribution to runoff on unpaved mountain roads: A case study in northern
951 Thailand. *Hydrol. Process.*, 15, 3203–3208.
952